

1 **Comparative genome analysis of *Enterococcus cecorum* reveals intercontinental spread of a**
2 **lineage of clinical poultry isolates.**

3
4 Jeanne Laurentie^{1,2}, Valentin Loux^{3,4}, Christelle Hennequet-Antier^{3,5}, Emilie Chambellon⁶, Julien
5 Deschamps¹, Angéline Trotereau⁶, Sylviane Furlan¹, Claire Darrigo⁶, Florent Kempf⁶, Julie Lao³,
6 Marine Milhes⁷, Céline Roques⁷, Benoit Quinquis⁸, Céline Vandecasteele⁷, Roxane Boyer⁷, Olivier
7 Bouchez⁷, Francis Repoila¹, Jean Le Guennec⁹, Hélène Chiapello³, Romain Briandet¹, Emmanuelle
8 Helloin⁶, Catherine Schouler⁶, Isabelle Kempf², and Pascale Serror^{1*}

9
10 ¹Université Paris-Saclay, INRAE, AgroParisTech, Micalis Institute, F-78350, Jouy-en-Josas, France

11 ² ANSES Laboratoire de Ploufragan-Plouzané-Niort, F-22440, Ploufragan, France.

12 ³Université Paris-Saclay, INRAE, BioinfOmics, MIGALE Bioinformatics Facility, F-78350, Jouy-en-
13 Josas, France.

14 ⁴ Université Paris-Saclay, INRAE, MaIAGE, 78350, Jouy-en-Josas, France

15 ⁵INRAE, Université de Tours, BOA, F-37380, Nouzilly, France.

16 ⁶INRAE, Université de Tours, ISP, F-37380, Nouzilly, France

17 ⁷ INRAE, Genotoul, GeT-PlaGe, F-31320, Castanet-Tolosan, France.

18 ⁸Université Paris-Saclay, INRAE, MGP, F-78350 Jouy-en-Josas, France.

19 ⁹Labofarm, F-22600, Loudéac, France.

20

21 *Corresponding author: pascale.serror@inrae.fr

22 Tel: +33134652166

23 Fax: +33134652065

24 **Running Title:** Comparative genome analysis of *Enterococcus cecorum*

25 **Key words:** *Enterococcus cecorum*, Comparative genomics, Avian pathogenesis, Antimicrobial
26 resistance, Poultry

27 **ABSTRACT**

28 *Enterococcus cecorum* is an emerging pathogen responsible for osteomyelitis, spondylitis, and
29 femoral head necrosis causing animal suffering, mortality, and requiring antimicrobial use in poultry.
30 Paradoxically, *E. cecorum* is a common inhabitant of the intestinal microbiota of adult chickens.
31 Despite evidence suggesting the existence of clones with pathogenic potential, the genetic and
32 phenotypic relatedness of disease-associated isolates remains little investigated. Here, we sequenced
33 and analyzed the genomes and characterized the phenotypes of more than 100 isolates, the majority of
34 which were collected over the last ten years in 16 French broiler farms. Comparative genomics,
35 genome-wide association study, and measured susceptibility to serum, biofilm forming capacity, and
36 adhesion to chicken type II collagen were used to identify features associated with clinical isolates.
37 We found that none of the tested phenotypes could discriminate origin of the isolates or phylogenetic
38 group. Instead, we found that most clinical isolates are grouped phylogenetically and our analyses
39 selected six genes that discriminate 94% of isolates associated with disease from those that are not.
40 Analysis of the resistome and the mobilome revealed that multidrug-resistant clones of *E. cecorum*
41 cluster in few clades and that integrative conjugative elements and genomic islands are the main
42 carriers of antimicrobial resistance. This comprehensive genomic analysis shows that disease-
43 associated clones of *E. cecorum* belong mainly to one phylogenetic clade.

44

45 **IMPORTANCE**

46 *Enterococcus cecorum* is an important pathogen in poultry worldwide. It causes a number of
47 locomotor disorders and septicemia, particularly in fast-growing broilers. Animal suffering,
48 antimicrobial use, and associated economic losses require a better understanding of disease-associated
49 *E. cecorum* isolates. To address this need, we performed whole genome sequencing and analysis of a
50 large collection of isolates responsible for outbreaks in France. By providing the first dataset on the
51 genetic diversity and resistome of *E. cecorum* strains circulating in France, we pinpoint an epidemic

52 lineage probably also circulating elsewhere and which should be targeted preferentially by preventive

53 strategies in order to reduce the burden of *E. cecorum*-related diseases.

54

55 INTRODUCTION

56 *Enterococcus cecorum* is a commensal bacterium of the gut microbiota of adult chicken (1-3). This
57 bacterium has emerged over the last twenty years as a significant cause of locomotor disorders in
58 poultry worldwide, particularly in fast-growing broilers (4). In France, reports on *E. cecorum* between
59 2006 and 2018 have shown an increase from 0.3% to more than 7% of total avian infections, the
60 majority of which include locomotor disorders in broilers (5). *E. cecorum* is mostly responsible for
61 osteomyelitis, spondylitis, vertebral osteoarthritis, and femoral head necrosis (1, 6, 7), causing
62 substantial losses in broiler production due to culling, mortality, condemnations at the slaughterhouse,
63 veterinary costs, and increased exposure to antibiotics (6, 8, 9). The development of *E. cecorum*
64 infections is multifactorial and depends on host genetics, rapid growth, feed composition, husbandry
65 procedures, and animal density in combination with the pathogenic potential of the bacterium (10-
66 13). The association between early intestinal carriage of *E. cecorum* and increased risk of infections
67 points to the gastro-intestinal tract as a route of infection (10, 11, 14, 15). Recent studies indicate that
68 lesion-associated *E. cecorum* isolates appear to be adapted to colonize the gut early in life, in contrast
69 to non-clinical isolates (i.e., strains isolated from the gut of healthy birds) that do not colonize to a
70 detectable level before week 3 (10, 14). It was also proposed that disinfection failure may contribute
71 to *E. cecorum* persistence and outbreaks due to biofilm formation (7, 16-18). Although suggested by
72 the prediction of host-binding proteins in the genome (19), the adhesion to host tissue proteins has
73 been overlooked and the robustness of *E. cecorum* biofilms and associated properties remain to be
74 investigated. It is also assumed that in Gram-positive bacteria, the thick layer of peptidoglycan that
75 surrounds the cytoplasmic membrane confers resistance to the bactericidal activity of the serum: for
76 instance, human serum selectively kills commensal *Enterococcus faecium* strains whereas disease-
77 associated *E. faecium* strains are not susceptible (20). Assessing the pathogenic potential of *E.*
78 *cecorum* isolates remains a challenge. Recently, an *in vivo* model has been used to distinguish the
79 pathogenicity between two clinical isolates under field conditions, but it is applicable to only a

80 limited number of strains (3). Less limiting, the chicken embryo lethality assay (CELA) has shown
81 tendencies where pathogenic strains kill more efficiently than commensal isolates (14, 21).
82 Several molecular epidemiological studies based on pulse-field gel electrophoresis (PFGE) patterns
83 of commensal and clinical isolates from the United States, Canada, Belgium, the Netherlands,
84 Germany, and Poland agree that commensal isolates have a higher diversity than clinical isolates,
85 suggesting the evolution of specific clones with higher pathogenic potential. However, clinical
86 isolates exhibited multiple PFGE patterns, supporting the hypothesis of the polyclonal nature of the
87 infectious isolates (22-26). Furthermore, repeated outbreaks with genotypically related isolates within
88 farms and local areas substantiate horizontal transmission and a farm-related reservoir (7, 17, 24, 26,
89 27). To date, only one complete genome of *E. cecorum* is available (type strain NCTC-12421
90 accession number NZ_LS483306.1) and only two comparative genomic studies of *E. cecorum*
91 isolates from the United States have been performed (19, 28). Comparison of partial genomes of three
92 commensal and three clinical isolates from the southeastern United States isolated between 2010 and
93 2011 indicated that the pathogenic *E. cecorum* strains had smaller genomes with more than 120 genes
94 absent or whose products had less than 40% identity in the commensal isolates (19). On the other
95 hand, ~70 genes of the non-clinical isolates were absent or encoded products with less than 60%
96 identity in the clinical isolates. In line with studies reporting a high rate of clinical isolates unable to
97 metabolize mannitol (14, 24, 25), the orthologs of mannitol phosphate dehydrogenase, the mannitol
98 operon activator, as well as the mannitol-specific component IIA of the phosphotransferase system
99 (PTS) were not found in clinical isolates. In another other study, partial genomes of nine clinical
100 isolates isolated in Pennsylvania in 2008 and 2009 were compared with those of nine non-clinical
101 isolates from the National Antimicrobial Resistance Monitoring System isolated between 2003 and
102 2010 (28). The trend of a slightly smaller genome size for clinical isolates was confirmed and
103 consistent with a larger accessory genome of non-clinical isolates. Noticeably, the non-clinical
104 genomes had more antibiotic resistance genes. By combining available *E. cecorum* draft genome

105 sequences (29, 30), the core genome was estimated to be 1,436 genes (28). Phylogenetic analysis of
106 the core genome led the authors to conclude that the isolates cluster independently of their clinical or
107 non-clinical status, which raises the question of whether the clinical isolates of *E. cecorum* belong to
108 specific genetic groups. The objective of this study was to provide a better insight on genomic
109 organization and phenotypic diversity of *E. cecorum* clinical isolates from broilers circulating
110 between 2007 and 2017 in Brittany, the leading French commercial broiler producing area. We
111 performed whole genome sequencing of more than hundred poultry and human clinical isolates in
112 order to better define the extent of genetic relatedness of clinical isolates and detect genes associated
113 with virulence-related traits. We completed this genomic analysis by testing isolates for their
114 adhesion to type II collagen, biofilm robustness, and growth in chicken serum. The overall genetic
115 diversity of *E. cecorum* was investigated by pan-genome analysis, with a particular focus on mobile
116 genetic elements (MGEs), antimicrobial resistance genes (ARGs), and genome-wide associations
117 (GWAS) between the accessory genes and the phenotypic traits.

118

119 **RESULTS**

120 *Clonality of E. cecorum clinical isolates*

121 To get insight into the gene repertoire of *E. cecorum*, we performed whole genome sequencing of 118
122 isolates, including 100 clinical isolates collected from 16 broiler farms in western France between
123 2007 and 2017, 6 clinical isolates of human origin, and 12 isolates from other studies that had been
124 previously sequenced (Table S1). 118 genomes sequenced by Illumina technology had a sequencing
125 coverage greater than 160X and an N50 between 62 kbp and 276 kbp (Table S2A). Hybrid assembly
126 of Illumina and Nanopore data of 14 genomes allowed the reconstruction of 10 complete genomes
127 (CIRMBP-1212, CIRMBP-1228, CIRMBP-1246, CIRMBP-1261, CIRMBP-1274, CIRMBP-1281,
128 CIRMBP-1283, CIRMBP-1287, CIRMBP-1292, and CIRMBP-1302) and improvement of genome
129 assembly completeness of 4 others (Table S2A). The estimated average length of the genomes is ~2.4

130 Mb and varies between ~2.05 and ~2.8 Mbp. Each genome had an average of 2,345 predicted protein
131 coding sequences (CDSs). A total of 277,011 CDSs were annotated. Comparison of the chromosomal
132 architecture of the 11 complete *E. cecorum* strains using NCTC12421 strain as reference revealed that
133 strain CIRMBP-1261 has a large chromosomal inversion of ~1.8 Mbp between the second and sixth
134 ribosomal RNA operon (Fig. S1). Strain CIRMBP-1287 also has a chromosomal inversion of 280 kbp
135 from genes DQL78_RS05120 to DQL78_RS06585, involving an insertion sequence (IS) of the IS3
136 family.

137 A further thirty available non-redundant *E. cecorum* genomes were included. These comprised
138 genomes of 9 clinical and 21 non-clinical isolates from Belgium, Germany, and the United States
139 (Table S2B). Comparative genomics analysis of the 351,733 CDSs from the 148 genomes identified
140 8,523 gene clusters in the pan-genome composed of a strict core-genome (present in all *E. cecorum*
141 genomes) of 1,207 CDSs, an accessory genome of 4,664 CDSs, and a unique genome of 2,652
142 (31.1%) CDSs (Fig. 1). The pan-genome curve displayed an asymptotic trend after the 140-genome
143 iteration, indicating a stabilization of the pan-genome within this dataset. Consistently, the core-
144 genome stabilized after the 125-genome iteration (Fig. 1A). These trends confirm that the genome
145 dataset used here provides a comprehensive overview of the gene repertoire of the *E. cecorum*
146 species. The distribution of the gene clusters revealed that ~47% of the pan-genome (n=3,979
147 including the unique genes) are present in one to three isolates (Fig. 1B), indicating that the genetic
148 diversity is partly attributable to gene acquisition. This hypothesis is further supported by a high
149 proportion (42%) of genes of unknown function.

150 The *E. cecorum* neighbor-joining (BioNJ) phylogenetic tree was constructed using the concatenated
151 sequence of the core genes (Fig. 2). The isolates clustered in five distinct phylogenetic clades (A to
152 E), supported by a bootstrap value of 100% and a higher maximum pairwise genetic distance between
153 clades (0.026 to 0.041) than within clades (<0.021) (Fig. S2). Clade E was further divided into 13
154 well-supported subclades (E1 to E13) with intra subclade pairwise genetic distances below 0.012,

155 indicating higher clonality of these isolates. Clades A to D contain 2 to 16 genomes, of which only
156 35% were avian clinical isolates. While clades B and D contain mainly genomes of non-clinical
157 isolates from the United States, clade A contains two European clinical human isolates and clade C
158 contains both non-clinical and clinical poultry isolates. In contrast, clade E comprises 117 genomes,
159 95% of which belong to avian clinical isolates from the United States, Belgium, Germany, Poland,
160 and France, suggesting a widespread-distribution of this clade. Of note, the type strain NCTC12421,
161 isolated from caecal content of a dead chicken from a farm in Belgium (1, 31) is part of subclade E3
162 and subclade E12 contains only avian isolates from the United States. Although the number of
163 isolates per subclade is limited, almost all isolates from subclades E6, E10, and E13 were isolated
164 after 2009 while those from subclades E4 and E11 were isolated before 2014 and after 2015,
165 respectively, indicating that the dominant subclasses have varied over the years. Due to sequence data
166 availability, single nucleotide polymorphism (SNP) analysis was only possible for genomes
167 sequenced in this study, thus excluding genomes from clades B, D and subclade E12. Of the 65,226
168 SNPs of the core-genome 2,443, 168, and 62 were specific to isolates of clades A (n=2), C (n=9) and
169 E (n=107), respectively. Of the thirteen non-synonymous clade E-specific SNPs, eight are non-
170 conservative and two are predicted as nonneutral in a phage shock protein (PspC, DQL78_RS04285
171 in NCTC12421) and ATP-binding cassette domain-containing protein (DQL78_RS04370 in
172 NCTC12421).

173 Altogether, these data revealed that clinical isolates of *E. cecorum* from poultry of different countries
174 are grouped phylogenetically and mainly belong to clade E, confirming their clonality and suggesting
175 either dissemination of well adapted clones or a convergent selection/adaptation to poultry genetics
176 and breeding methods.

177
178 *Six genes, significantly associated with origin, differentiate avian clinical from non-clinical isolates*
179 *in the 148 genomes*

180 To further explore the genetic basis for the epidemic success of the *E. cecorum*, clade E isolates we
181 searched for genes significantly associated with clade membership. The majority of unique genes
182 (71.9%) are carried by isolates from clades A, B, C and D, indicating a higher genetic diversity in
183 these clades. However, this trend may result from the enrichment of the collection in clade E isolates.
184 Consistently, we identified 97 accessory genes significantly associated with clade E isolates (Table
185 S3). The most abundant group of the 83 clade E-enriched genes after the unclassified hypothetical
186 protein-encoding genes (n=17) are predicted carbohydrate metabolism and transport (n=13) genes and
187 cell wall/membrane/envelop biogenesis genes (n=12). A high proportion of the clade E-enriched
188 genes are clustered loci, including the capsule polysaccharide (CPS) biosynthesis locus (from
189 CIRMBP1228_00568 to CIRMBP1228_00581 in strain CIRMBP-1228), a large gene cluster
190 comprising biotin biosynthesis genes (CIRMBP1228_01807 to CIRMBP1228_01837), and one
191 putative operon of carbohydrate metabolism (CIRMBP1228_02727 to CIRMBP1228_02733).
192 Alignment of gene products of the representative capsule biosynthesis loci from the complete
193 genomes identified two closely related loci represented by genomes of CIRMBP-1228 and CIRMBP-
194 1212 (Fig. S3) that account for 66.7 and 14.5% of the clade E isolates, respectively. The remaining 14
195 genes significantly associated with origin of the isolates (clinical and non-clinical poultry isolates or
196 clinical human isolates) are predominantly absent in clade E-isolates. They include genes encoding a
197 pseudouridine synthase (CIRMBP1294_00547), a predicted nucleotide sugar dehydrogenase
198 (CIRMBP1294_00386), a diacylglycerol kinase family lipid kinase (CIRMBP1294_00623), and two
199 stress-related proteins (CIRMBP1294_00560 and CIRMBP1294_00758). In line with the large
200 proportion of clade E clinical isolates in the collection, 30 clade E-enriched genes are also enriched in
201 clinical poultry isolates compared to non-clinical poultry and clinical human isolates (Table S4A).
202 They include genes of the CPS biosynthesis locus (CIRMBP1228_00573, CIRMBP1228_00574,
203 CIRMBP1228_00575), 27 genes of the biotin gene cluster, and an H protein gene of the glycine
204 cleavage system generally involved in protein lipoylation. A total of 65 genes are significantly

205 associated with the origin of the isolates. In addition to those enriched in clade E isolates, other genes
206 enriched in avian clinical isolates encode a phosphoenolpyruvate:carbohydrate phosphotransferase
207 system (PTS), a transketolase (CIRMBP1228_00604 to CIRMBP1228_00607), as well as proteins of
208 unknown function. Although no specific gene signature for avian clinical isolates was found, we
209 identified 6 accessory genes (CIRMBP1228_00573, CIRMBP1228_00586, CIRMBP1228_00757,
210 CIRMBP1228_01816, CIRMBP1228_02735, and CIRMBP1283_01819) that allow to identify 94 %
211 of avian clinical isolates (Table S4B). With the exception of seven avian clinical isolates from clades
212 C or D, all other genomes of clinical isolates have an average of 4 selected genes (range from two to
213 six genes), while non-clinical isolates have one gene at most. We also found twelve genes that may be
214 enriched in clinical human isolates. These include 8 genes predicted to be involved in import and
215 utilization of ascorbate in anaerobic conditions (32, 33).

216 Despite the difficulty in identifying genes specific to the origin of the isolates, this work highlights
217 six genes coding a glycosyltransferase (CIRMBP1228_00573), two PTS EIIc components
218 (CIRMBP1320_01424, CIRMBP1228_02735), and three hypothetical proteins
219 (CIRMBP1228_00586, CIRMBP1228_01816, CIRMBP1228_00757) that can discriminate most of
220 the isolates associated with poultry disease from those that are not.

221

222 *Multiresistant clones of E. cecorum cluster in few clades*

223 Next, we searched the 148 sequenced genomes for the presence of acquired ARGs using ResFinder,
224 BLAST and the PLSDB database. A total of eighteen ARGs were identified (Fig. 3). Tetracycline and
225 macrolide-lincosamide-streptogramin B (MLS) resistance genes were detected in 95% and 75% of the
226 isolates, respectively. In total, 70% of the genomes had at least one gene for resistance to these two
227 families of antimicrobials, with *tet(M)* and *erm(B)* being the most prevalent. Resistance genes to
228 other antimicrobial classes such as aminoglycosides (10%), bacitracin (30%), and vancomycin (0.6%)
229 were also detected. Only two isolates (CIRMBP-1244 and CIRMBP-1314) did not contain any ARG

230 searched. Overall, thirty-nine genomes carried genes conferring resistance to three antimicrobial
231 families and seven genomes had at least four genes for resistance to different antimicrobial families
232 (Fig. 3). The most common combinations of ARGs in multidrug resistant isolates cover the
233 tetracycline and MLS families in combination with aminoglycosides in clades C and D or with
234 bacitracin in clades C and D, and subclades E10, E11 and E12. Aminoglycoside resistance genes are
235 carried by non-clinical genomes with an enrichment in U.S. strains. The near-systematic presence of
236 ARGs in the genomes of *E. cecorum* isolates suggests that the species may have undergone strong
237 selection for antibiotics, tetracyclines and MLS in particular, but that these two antibiotic resistances
238 did not provide a selective advantage to clinical isolates.

239 Several *E. cecorum* genome regions carrying ARGs conserved in Gram-positive bacteria were
240 identified in the PLSDB database, but none was encoded by a previously identified plasmid. Their
241 analysis highlighted different ARGs clusters. They comprised *erm(B)*, *vat(D)*, and *msr(D)* genes,
242 *tet(L)*, *tet(M)*, and *bcr* genes or *tet(L)*, *tet(M)*, *ant(6)*, and *bcr* genes. Further characterization of the
243 vancomycin resistance operon carried by strain CIRMBP-1294 revealed that the *vanA* operon was
244 integrated into the chromosome 12 kbp away from the genes that confer resistance to narasin and to
245 erythromycin in between (Fig. S4). This chromosomal region was closely related to that of the *E.*
246 *faecium* plasmid pVEF3 (34) identified in broiler isolates from Sweden (35) and was flanked by two
247 transposase genes of the IS3 family. However, no conjugative or mobilization element was detected
248 close to this ARG cluster. Although about twenty plasmid-related gene families were identified in the
249 pan-genome, a single putative 4.4 kbp plasmid was detected in the complete genome of strain
250 CIRMBP-1292 and 6 other isolates (CIRMBP-1233, CIRMBP-1259, CIRMBP-1286, CIRMBP-1289,
251 and CIRMBP-1304), but no ARG was detected on this small plasmid. Together, these results suggest
252 that plasmids are rare in this bacterial collection and ARGs are encoded on mobile genomic islands.

253

254 *E. cecorum mobilome is a major contributor to inter- and intra-clade diversity*

255 In Gram positive bacteria, ARGs and related transposons are frequently integrated in complex MGEs
256 forming Integrative Conjugative Elements (ICEs) or Integrative Mobilizable Elements (IMEs) that
257 may be difficult to identify in draft genomes (36). To evaluate the contribution of these elements to
258 the spread of ARGs and to *E. cecorum* genome diversity, we predicted ICEs and IMEs in the eleven
259 complete genomes and the two large contigs of genome CIRMBP-1320 using ICEScreen (J. Lao, T.
260 Lacroix, G. Guédon, C. Coluzzi, N. Leblond-Bourget, and H. Chiapello, submitted for publication).
261 ICEScreen ICE and IME detection relies on the presence of Signature Protein CDSs (integrase,
262 coupling protein, relaxase, and virB4) grouped on the genomes and previously shown to be a valuable
263 clue to the presence of an integrative element (37, 38). ICEs were defined by the superfamily and
264 family of their signature proteins (37). Each *E. cecorum* genome contained at least one ICE (Table
265 S5A and Fig. 4). In total, thirty-three mobile genetic elements including five types of ICEs (belonging
266 to the Tn916, Tn5252, and TnGBS1 superfamilies), two IMEs, three Tn917, and one partial
267 conjugative element were identified. Their size ranged from ~5 kbp for Tn917 to ~103 kbp for the
268 TnGBS1 ICE of genome CIRMBP-1302. The Tn916 ICE of genomes CIRMBP-1228 and CIRMBP-
269 1281, integrated upstream of the 30S ribosomal protein S6 encoding gene, included another ICE of
270 undescribed family encoding a DDE transposase, a MobC-like relaxase, a VirD4-like coupling
271 protein, and a type IV secretion system (T4SS) protein VirB4. We also investigated the presence of
272 other genomic islands (GIs) in the complete genomes (Fig. 4, Table S5B). A total of 42 GIs were
273 identified, with a size ranging from ~8 kbp to ~122 kbp for the complex GI that comprises an ICE
274 (Tn916, ICEBs1, ICESt3) in genome CIRMBP-1228. Each genome harbored from 3 ICE-related
275 elements or genomic elements (strain CIRMBP-1212 of subclade E5) up to 12 (strain CIRMBP-1228
276 of subclade E4). They were mainly integrated in intergenic regions or the 3'-end of genes with no
277 effect on the encoded sequences. As expected, all Tn917 and ICEs of the Tn916 family encoded
278 *erm*(B) and *tet*(M), respectively. Other ARGs such as *tet*(L), *tet*(O), *ant*(6), and the *bcr* operon were
279 carried on Tn916-related ICEs or on GIs. Besides genes involved in GI transfer, a few had predicted

280 functions related to biotin biosynthesis, restriction modification enzymes, cadmium/arsenate
281 resistance, toxin-antitoxin systems, redox enzymes, type 2 secretion system, and flagella and
282 chemotaxis. Analysis of the distribution of the ICE-related elements and the GIs in the other 136 *E.*
283 *cecorum* genomes (Table S5B) revealed three highly dispersed elements: the Tn916-related ICE of
284 strain CIRMBP-1292 in 113 genomes, the GI inserted near the *rpsB* gene and encoding the biotin
285 biosynthesis genes found in 90 genomes, and the transposon Tn917 in 65 genomes (Table S5B). The
286 GI inserted between *dnaX* and *sufB* of strains CIRMBP-1287 and CIRMBP-1274 was highly
287 prevalent in subclades E6 and E10, respectively. The same is true for the cognate element of
288 CIRMBP-1283 and CIRMBP-1302 that is detected in all isolates of subclade E11, to which
289 CIRMBP-1283 belongs. Other elements are enriched in specific subclades, such as the GI near the
290 23S rRNA methyltransferase *rlmD* gene and ICEs of the Tn*GBS1* and Tn916 families of CIRMBP-
291 1274 enriched in subclade E6, the ICE of Tn916 family of CIRMBP-1212 enriched in subclade E13,
292 the GI inserted in the 3'-end of CIRMBP1228_01030, and the ICE of the Tn*GBS2* family of
293 CIRMBP-1228 close to the gene CIRMBP1228_01622 enriched in E4. According to their gene
294 content, fifteen elements appear to be more strain-specific in strains CIRMBP-1320 (n=4), CIRMBP-
295 1281 (n=4), CIRMBP-1292 (n=3) and NCTC12421 (n=4). Although the genomes used to identify
296 ICEs and GIs are not representative of all clades, homologs were found in almost all clades except
297 clade B, which gathers only five non-clinical poultry isolates from the United States. Yet However,
298 these genomic elements were less conserved in isolates from the United States, suggesting they were
299 acquired independently. We conclude that the majority of the identified ICEs and GIs are enriched in
300 some clades, while only a few are shared across clades.

301 As prophages are easier to detect than GIs and mobile genetic elements, prophages were searched for
302 in all *E. cecorum* genomes sequenced, including NCTC12421. A total of 103 complete prophages and
303 30 incomplete prophages were identified in 78 (66.1 %) *E. cecorum* genomes (Table S6). Prophage
304 size ranged between 31 and 59 kbp in length. The prophages were related to 19 different types that

305 varied across the phylogenetic groups. The subclade E4 was enriched with prophages related to
306 *Faecalibacterium* phage oengus (39) that was the most commonly found (n=31), followed by
307 prophages related to the *Siphoviridae* temperate phage EFC-1 of *Enterococcus faecalis* (40) (n=16).
308 Prophages related to the *Myoviridae* temperate bacteriophage EJ-1 of *Streptococcus pneumoniae* (41)
309 (n=13) were mostly found in genomes of subclade E10 while those related to the *Siphoviridae*
310 temperate phage of *Lactococcus lactis* 50101 (n=12) were most prevalent in subclade E6. Conversely,
311 clade C had the most diverse prophages and subclades E10 and E12 contained the least number of
312 prophages. Prophages related to *Siphoviridae* temperate phage 5093 of *Streptococcus thermophilus*
313 (42) (n=9) were identified in several phylogroups. A total of 13 different integration sites for
314 temperate bacteriophages were identified, mainly in intergenic regions and at the 3' end of genes
315 without changing the reading frame (Table S6). However, the prophage related to
316 PHAGE_Strept_EJ_1_NC_005294 integrated in the PreQ1 riboswitch is likely to change the
317 expression of the downstream nucleoside hydrolase gene. Like ICEs and GIs, prophages are less
318 prevalent in the ~700 kbp surrounding the origin of replication of the chromosome (Fig. 4), indicating
319 that mobile genetic elements are not randomly distributed in the *E. cecorum* genome.

320
321 *Biofilm robustness, adhesion to type II collagen, and growth in chicken serum are not associated with*
322 *gene content.*

323 To get phenotypic insight into the 118 isolates, we independently examined phenotypes relevant to *E.*
324 *cecorum* pathogenesis: biofilm robustness, adhesion to type II collagen, and growth in chicken serum
325 (see methods in the supplemental material). Hierarchical clustering of these phenotypes (Fig. 5)
326 revealed 17, 11 and 9 groups of strains for biofilm robustness, type II collagen adhesion, and growth
327 in chicken serum, respectively. The lack of concordance between these phenotypic groups and clades
328 strongly suggests that none of the phenotypes are discriminating between clades. In an attempt to rank
329 isolates, the most robust biofilm-forming isolates were CIRMBP-1302 (subclade E13), CIRMBP-

330 1277 (clade C) and CIRMBP-1228 (subclade E4) and the most fragile biofilm-forming isolates were
331 CIRMBP-1204 (subclade E1), CIRMBP-1205 and CIRMBP-1211 (subclade E4), and CIRMBP-1225
332 (subclade E6). The most collagen-adherent isolates were CIRMBP-1274 (subclade E6) and CIRMBP-
333 1277 (clade C). All of the *E. cecorum* isolates had a serum growth index below the index of the
334 *Escherichia coli* control strain sensitive to the bactericidal effect (190.34 +/- 123.88) of the serum and
335 in the range of the non-sensitive *E. coli* control strain (3.172 +/- 4.2). The *E. cecorum* isolates with
336 the lowest indexes were strains CIRMBP-1318 (0.229 +/- 0.21) and CIRMBP-1206 (0.467 +/- 0.001)
337 belonging to subclades E3 and E4, respectively. The *E. cecorum* strains with the highest indexes were
338 strains CIRMBP-1312 (3.85 +/- 0.44) of subclade E12, CIRMBP-1197 (4.21 +/- 2.2) of clade A, and
339 CIRMBP-1298 (5.71 +/- 2.9) of subclade E10. Taken together these results indicate that the growth of
340 *E. cecorum* is not affected by the presence of chicken serum. Beside strain CIRMBP-1277, which
341 formed strong biofilms and had a high capacity to adhere to collagen, no relationship between the
342 expression of the three phenotypes and adherence to collagen was observed. Moreover, no accessory
343 genes were associated with the phenotypic groups or with binary transformed values, suggesting
344 functional redundancy between genes and/or differential gene expression between isolates.

345
346 *Clinical isolates of E. cecorum show a broad spectrum of virulence in chicken embryos*

347 To evaluate the pathogenic potential of *E. cecorum* strains isolated from diseased broilers in French
348 farms, we used the chicken embryo lethality assay (CELA) reported by Borst et al. using strain
349 CIRMBP-1309 (original name CE3) and strain CIRMBP-1311 (original name SA2) as biological
350 controls for a non-pathogenic and pathogenic poultry isolate, respectively (21). We tested the 11 *E.*
351 *cecorum* strains with the most complete genomes (see methods in the supplemental material). No
352 embryo died in the control group. The two *E. cecorum* control strains behaved as expected: 53 % of
353 the embryos were still alive 6 days after inoculation with the commensal strain CIRMBP-1309,
354 whereas 100% of embryos died after 2 days when inoculated with strain CIRMBP-1311 isolated from

355 spondylitis lesions (Fig. 6). Strain CIRMBP-1294, isolated from infected vertebrae and strain
356 CIRMBP-1320, isolated from human infection induced less than 27% embryonic lethality, indicative
357 of a low virulence in CELA. In contrast, strains CIRMBP-1228, CIRMBP-1274, CIRMBP-1292,
358 CIRMBP-1302, and CIRMBP-1304, mainly isolated from infected vertebrae, showed the same
359 virulence as strain CIRMBP-1311 with an overall average lethality of 85% at day 2 post-infection.
360 They thus could be considered as virulent isolates. The lethality of strains CIRMBP-1212, CIRMBP-
361 1281, CIRMBP-1283, and CIRMBP-1287 was intermediate and higher than observed for the least
362 virulent strains CIRMBP-1294 (p-values between 0.026 and 0.064) and CIRMBP-1320 (p-values
363 between 0.026 and 0.073). Close analysis of the gene content in the 10 strains exhibiting virulence
364 and in the three strains considered as non-virulent in CELA identified 33 genes, of which 18 were
365 already found enriched in clade E isolates and 6 in avian clinical isolates. Predicted function for these
366 genes indicates a bias in favor of carbohydrate transport and metabolism (Table S7).
367 In line with data obtained for biofilm robustness, binding to collagen, and growth in chicken serum,
368 the clear gradient of virulence observed in the CELA for clinical isolates, supports the hypothesis of
369 the multifactorial nature of *E. cecorum* pathogenesis.

370

371 **DISCUSSION**

372 *E. cecorum* has emerged as an opportunistic pathogen in poultry worldwide. The present study shows
373 the clonality of a large collection of clinical *E. cecorum* isolates collected between 2007 and 2017 in
374 the leading French commercial broiler producing area. It identifies main phylogenetic clades and
375 subclades and provides a first insight into the intercontinental clonality of clinical isolates of *E.*
376 *cecorum* from poultry. Six genes significantly associated with the origin of the isolates allow to
377 discriminate 94% of the avian clinical isolates of the collection from the non-clinical ones. Based on
378 new complete genomes, we also provide insight into the diversity of the mobile genetic elements of
379 *E. cecorum* that carry ARGs.

380 One way of assessing the diversity of a species is to analyze its core- and accessory-genomes (43-45).
381 Although it should be considered as rough estimates due to the use of draft genomes, the current *E.*
382 *cecorum* core-genome represents only 14.1% (1,207/8,523 CDSs) of the pan-genome and ~50% of
383 the average *E. cecorum* genome. While the size of the core-genome is within the range of the one
384 reported by Sharma et al., the *E. cecorum* pan-genome is now 35% larger than in earlier estimates due
385 to the addition of 130 genomes to the 18 genomes previously used (28). The increase in genome size
386 corresponds to an average of only 20 genes per genome; however, the low gene discovery rate is
387 probably due to the high proportion (93%) of clinical poultry isolates in clade E. Indeed, clade E
388 isolates (n=117) accounted for 22% (1,873/8,523) of accessory genes while more distantly related
389 isolates of clades A (n=2), B (n=5), C (n=16) and D (n=8) accounted for 34.0% (2,897/8,523) of
390 accessory genes. The proportion of core genes and accessory genes strongly correlates with the
391 lifestyle of the bacterium. A small core-genome compared to a large pan-genome reflects the
392 diversity of hosts and lifestyles, as observed in *E. coli sensu stricto* and *Salmonella enterica*, two
393 ubiquitous species with commensal or pathogenic lifestyles, whose core-genome accounts for 0.39%
394 and 1.9% of the pan genome, respectively (46, 47). Conversely, a high proportion of core genes
395 reflects more restricted lifestyles, such as those of *Bacillus anthracis* (65%), an obligate pathogen and
396 *Staphylococcus aureus* (36%) and *Streptococcus pyogenes* (37%), two human-restricted pathogens
397 (44). Broader sampling from different hosts and countries is needed to further evaluate the diversity
398 of the *E. cecorum* species.

399 Genome reduction associated with pathogenicity is observed in many bacteria, including
400 *Streptococcus suis* and *Streptococcus agalactiae* whose genome size is reduced in virulent host-
401 adapted isolates (48-51). Although longer *E. cecorum* genomes belonged to clinical poultry isolates,
402 the average genome size was similar for all poultry isolates regardless of their clinical status
403 (2.40±0.14 and 2.36±0.11 Mbp for clinical poultry isolates and non-clinical poultry isolates,
404 respectively). This observation differs slightly from two previous studies on isolates from the United

405 States, where clinical isolates had shorter genomes than non-clinical isolates (19, 28). The latter is
406 most likely due to the small number of genomes examined and the sampling of clinical isolates,
407 which according to our findings belong all to the same phylogenetic subclade E12. In the current
408 dataset, the smallest genomes correspond to isolates from phylogenetic subclade E11 and the largest
409 genomes to isolates from subclade E4. Interestingly, all but one E4 genomes (n=27) have no
410 CRISPR-*cas* systems, correlating with abundant ICEs, GIs and prophages.

411 Previous molecular studies, using mainly PFGE, have converged towards the genetic homogeneity of
412 *E. cecorum* clinical isolates from the same country compared to non-clinical isolates (19, 22-28).
413 Despite more than 6,500 cases of *E. cecorum* infections in poultry reported in France since 2007 (52),
414 the genetic diversity of *E. cecorum* in France and genetic relatedness with isolates from other
415 countries have never been studied. Phylogenetic analysis of 100 isolates spanning the period from
416 2007 to 2017 showed that a single clade (E) was responsible for almost all (96%) cases in farms
417 between 5 and 90 km apart in Brittany. The phylogenetic congruence of clinical isolates from the
418 United States is consistent with two hypotheses: i) isolates were issued from a transcontinental
419 dissemination or ii) isolates from different regions suffered comparable selective pressure. The use of
420 a limited number of commercial genetic lines of broiler chickens may have contributed to the
421 selection of *E. cecorum* clones with pathogenic potential and allowed transcontinental dissemination.
422 While the hypothesis of a transcontinental spread of clade E isolates through the meat trade is
423 unlikely, trade in live animals (53), surface-contaminated eggs, or transport by wild birds may well
424 have contributed to this spread. The second hypothesis, although less likely, is a parallel convergent
425 selection due to breeding conditions. The isolates in this study may not represent the full diversity of
426 the French clinical population of *E. cecorum*; however, their temporal distribution reflects the spread
427 and persistence of a clade particularly adapted to broilers with the emergence over time of some more
428 successful subclades. This is illustrated by the dominance of subclade E4 (82%) in France and
429 subclade E12 (75%) in the United States between 2008 and 2010 in the current dataset. Subsequently,

430 the dominant subclades were E6, E13, E11 and E10, the latter two were dominant on French farms in
431 2016. The temporary circulation of specific subclades may be due to natural evolution or adaptive
432 changes in response to modifications of breeding practices (like novel biocides and cleaning
433 procedures, different feed origin, composition, or additives), but the reasons remain to be determined.
434 Though less frequent, clinical isolates were also found in clades C and D, which contain non-clinical
435 isolates and display higher diversity. Noticeably, isolates of these two clades have multiple ARGs,
436 which may confer selective advantage and thus contribute to the pathogenic potential in specific
437 conditions that remain to be determined. Additional genomes of non-clinical isolates, but also clinical
438 isolates from diverse countries and other poultry species and husbandry systems are required to obtain
439 a comprehensive view of the *E. cecorum* population structure and determine whether *E. cecorum*
440 clade E isolates are broiler specific.

441 *E. cecorum* has been occasionally involved in human infections (54-56). Four of the six clinical
442 human isolates of this study were clade E isolates, supporting a poultry origin. However, this does not
443 lead to the conclusion that the contamination was food-borne. The two other clinical human isolates
444 belong to clade A and are phylogenetically close. Both have large clusters of highly specific genes,
445 including an iron transporter and a ~60 kbp motility locus characterized by flagella and chemotaxis
446 genes, which may have been acquired by horizontal gene transfer from other species of enterococci,
447 such as *E. casseliflavus*, *E. gallinarum*, or *E. columbae* encountered in birds, but also in other animals
448 including humans, insects, and aquatic hosts for the first two (57).

449 The dominance of *E. cecorum* clinical isolates from clade E strongly supports the hypothesis that
450 clade E isolates have acquired properties increasing their fitness and/or infectivity. At the core-
451 genome level, all clade E isolates share common SNPs that may confer a selective advantage in the
452 host. Of the two non-neutral mutations one is in the phage shock protein gene *pspC* that encodes an
453 ortholog of the transmembrane protein LiaY, probably involved in resistance to cationic antibiotics
454 and antimicrobial peptides (58). Codon changes leading to synonymous SNPs may also modify the

455 translation efficiency as such to foster cell fitness (59). In addition to the clade E-specific mutations
456 in the core genes, 83 accessory genes were found enriched in the clade E isolates of which thirteen
457 genes of the capsule operon. The capsule is an important virulence factor to evade host immunity,
458 including for enterococci (see (60) for a review on the subject). We identified two closely related
459 capsule loci in 81.2% of the clade E isolates. The strong association between these capsule loci and
460 the clinical isolates suggests a role in virulence, probably by promoting immune evasion (61).
461 However, virulence, especially for opportunistic pathogens, is a multifactorial process involving
462 multiple bacterial traits such as metabolic functions and stress resistance (62, 63). Other clade E
463 enriched genes may confer *E. cecorum* alternative metabolic capacities to survive and/or multiply in
464 the host. The predicted galactitol phosphotransferase system (CIRMBP1228_02729 to
465 CIRMBP1228_02731) and galactonate catabolism enzymes (CIRMBP1228_02728, and
466 CIRMBP1228_02732), as well as the biotin biosynthesis genes may give *E. cecorum* an advantage in
467 competing with commensal species in nutrient-limited environments such as the gastro-intestinal
468 tract, considered as a portal of entry during the first week of life of the host (10). Of note, the
469 mannitol-1-phosphate 5-dehydrogenase (*mtlD*) gene proposed to be specific of non-clinical isolates
470 (19) was not discriminant between non-clinical and clinical poultry isolates of our collection because
471 it is present in only seven isolates from different origins. Conversely, we selected 6 genes, which
472 taken together allow to discriminate more than 90% of the clinical isolates. The combined detection
473 of these candidate genes on a larger collection of clinical and non-clinical isolates is necessary in
474 order to evaluate their use for the detection of early carriage of potentially pathogenic isolates,
475 particularly during the first week of life. In contrast, while ascorbate catabolism genes are dispensable
476 in 70% of clinical avian isolates, they may confer a competitive advantage to avian non-clinical
477 isolates and human clinical isolates.

478 MGEs including prophages are major contributors to the evolution of the gene repertoire. We
479 identified 75 MGEs corresponding to predicted ICEs or related elements and GIs in the complete

480 sequenced genomes and a total of 105 complete prophages in the 118 sequenced genomes. Three GIs
481 have a composite structure with phage genes and more than one integrase gene, likely resulting from
482 independent integration of different MGEs (37, 64). *E. cecorum* MGEs are integrated in the 3' end or
483 in intergenic regions of genes encoding a ribosomal protein (*rpsB*, *rpsI*, *rpsF*, or *rpmE*), in a few
484 tRNA genes or riboswitches (*tRNA-Thr*, *tmRNA*, *preQ1*), but also in various other intergenic regions.
485 This is consistent with the different site-specificity of the prevalent integrases of the tyrosine and
486 DDE recombinase families (36-38), although there is relatively little integration in the tRNA genes
487 that are frequently targeted by tyrosine integrases in streptococci (65). The apparently non-random
488 distribution of the *E. cecorum* MGEs integrated relatively far away from the chromosomal origin of
489 replication may relate to the eviction of highly expressed genes located near the origin of replication
490 (66, 67). Among the prophages we identified, prophages homologous to PHAGE_Strept_5093,
491 PHAGE_Enterо_EFC_1, and PHAGE_Bacill_phBC6A52 were also detected in clinical and non-
492 clinical poultry isolates from the United States (28). In contrast, and with the exception of Tn917, the
493 ICEs and GIs identified in the French isolates are not well conserved in the U.S. isolates, indicating
494 that they were acquired separately and contribute to local adaptation. In addition to the type IV
495 secretion system involved in the formation of the DNA translocation channel, ICEs encode cell
496 surface adhesins for attachment to the target cell. These include LPxTG cell wall-anchored adhesins
497 such as *S. agalactiae* antigen I/II family adhesins also referred to as group B *Streptococcus* surface
498 proteins (Bsp) (68, 69). These structural proteins were also shown to promote biofilm formation,
499 interaction with host cells, and virulence (70, 71). We identified Bsp-like proteins in TnGBS1 and
500 TnGBS2-related ICEs, proteins containing Cna B domains initially found in microbial surface
501 components recognizing adhesive matrix molecules (MSCRAMMs), and VaFE repeat-containing
502 surface-anchored proteins in diverse *E. cecorum* ICEs and GIs. Yet none of these associated with a
503 specific trait or origin. However, the variability of these adhesins may hinder any association, as they
504 may also compensate each other. ICEs and GIs may carry diverse genes, known as cargo genes, that

505 are not involved in gene transfer, but may confer a selective advantage to the host strain. We have
506 identified several *E. cecorum* cargo genes encoding toxin-antitoxin modules that function as MGE
507 addiction systems but are also involved in the control of bacterial growth (72). Other cargo genes
508 encode restriction-modification systems that protect the cell against horizontal gene transfer or are
509 genes involved in protection against oxidative stress, or in resistance to cadmium or arsenate, which
510 could confer a better fitness contributing to ecological adaptation. An accessory SecA2-SecY2 operon
511 was also identified in strain CIRMBP-1228. Such systems are dedicated to the export of glycosylated
512 serine-rich repeat proteins (SRRPs) that participate in adhesion to host cells and/or in biofilm
513 formation (73, 74). Functional analysis on a few selected strains is required to evaluate whether and
514 how these accessory genes contribute to adaptation to environmental challenges.

515 ARGs are other clinically important cargo genes spread by ICEs and GIs (75). The ARGs identified
516 in *E. cecorum* confer resistance to tetracycline, macrolides, bacitracin, aminoglycosides, and much
517 more rarely to glycopeptides. The most prevalent are *tet(M)*, *tet(L)*, and *erm(B)* genes. This is in line
518 with the high prevalence of resistance to tetracycline and erythromycin in *E. cecorum* found in
519 various studies, as reviewed by Jung et al. (12) and with the use of tetracyclines and macrolides
520 despite substantial efforts to reduce their use in veterinary medicine. As anticipated from the
521 literature, *tet(M)* is carried on ICEs of the Tn916 family and *erm(B)* on Tn917 (76). Other macrolide
522 resistance genes, such as *mef(A)*, *msr(D)*, or *lnu(B)* and the aminoglycoside resistance genes, such as
523 *ant(6)-Ia* and *aph(3')-III* are prevalent in the ~~USA~~ U.S. isolates (28). *mef(A)*, *msr(D)*, *vat*, and *erm(C)*
524 genes are located on the same GI in CIRMBP-1246 (CIRMBP1246_01012-CIRMBP1246_01050),
525 *lnu(C)* is adjacent to the IS1595 family transposase ISSag10 and the two adjacent genes *lnu(B)* and
526 *lsa(E)* are next to the IS1595 family transposase ISCpe8, previously described in an avian
527 *Clostridium perfringens* strain carrying the lincomycin resistance gene *lnu(P)* on the plasmidic
528 transposable tISCpe8 (77). Another prevalent ARG is the bacitracin resistance operon *bcr* in isolates
529 of clades C, D, and subclades E10, E11, and E12. This operon is frequently associated with *tet(M)*

530 and *tet(L)* genes on ICEs of the Tn916 family. The highly conserved nucleotide sequence of the *bcr*
531 operon, including the flanking *ISEnfa1* and its location on Tn916-like elements or GIs, is consistent
532 with avian inter-species transmission involving *E. faecalis*, *E. faecium* and *C. perfringens* (78, 79).
533 Note that the carriage of *tet(M)* and *tet(L)* on the same Tn916-like element is uncommon. It was first
534 described in *Streptococcus gallolyticus* and proposed to benefit the host bacterium under stressful
535 conditions (80, 81). A single clinical poultry isolate from France has the *vanA* operon, a gene already
536 described in an *E. cecorum* strain from retail poultry in Japan (82). Overall, 26% (n=39) of isolates
537 encode multiple ARGs (4 to 10) conferring resistance to at least three antimicrobial families, and are
538 prevalent in clinical and non-clinical isolates of clades C, D, and in subclades E11 and E12. The very
539 few strains without predicted ARG and the differential ARG profiles between French and U.S.
540 isolates probably reflect a strong antibiotic selective pressure that differs between the two countries.
541 Indeed, in-feed bacitracin and in-feed macrolides are still used in poultry farming in the United States
542 (83). The successive European bans of antibiotics (avoparcin in 1997, bacitracin, spiramycin, tylosin,
543 and virginiamycin in 1999, avilamycin and flavophospholipol in 2006) and the French national
544 EcoAntibio plans (84, 85) launched in 2012 and 2017 to fight antimicrobial resistance in animal
545 health and promote the responsible use of antibiotics might have contributed to contain the spread of
546 ARGs and reduce MLS resistance genes as observed in the recent isolates of subclade E10. In fact,
547 this is in line with the decreasing trend of macrolide resistance of *E. cecorum* strains isolated in
548 French poultry according to the French surveillance network for antimicrobial resistance in bacteria
549 from diseased animals (RESAPATH on line, <https://shiny-public.anses.fr/resapath2/>). However, there
550 has been a marked increase in bacitracin resistance genes in French isolates since 2015, even though
551 bacitracin is not used in avian veterinary medicine in France (86). Bacitracin is produced by *Bacillus*
552 *licheniformis* and *Bacillus subtilis* strains. With the need for alternatives to antibiotics in livestock,
553 bacilli strains are used as probiotics or applied together with lactic acid bacteria as protective biofilm
554 against pathogens (87-89). The increase of *E. cecorum* isolates carrying the *bcr* operon points to the

555 need for examining whether *Bacillus* strains applied in farms produce bacitracin or related
556 antimicrobial compounds that could contribute to the dissemination of the *bcr* operon. Reassuringly,
557 relatively few aminoglycoside and vancomycin resistance genes that target gentamicin and
558 glycopeptides, two critically important antimicrobials in human medicine, are found in French
559 isolates, as elsewhere in Europe (12).

560
561 Overall, the results of this study shed light on the population of *E. cecorum* clinical isolates in France
562 and reveal a genetic linkage with *E. cecorum* clinical isolates from elsewhere. We have shown that,
563 based on the available data, the majority of clinical poultry isolates are phylogenetically distinct from
564 non-clinical poultry isolates and form a main clade responsible for the outbreaks of *E. cecorum* in
565 France and probably in the United States and Europe. ICEs and GIs are the main carriers for
566 antimicrobial resistance. The E clade of *E. cecorum* appears to have adapted to the conditions under
567 which poultry is reared, highlighting its importance as an emerging threat to the poultry industry
568 worldwide. This information can be used to design and guide preventive strategies to reduce the
569 impact of *E. cecorum* clade E isolates.

570

571 MATERIAL AND METHODS

572 *Bacterial strains*

573 A total of 118 strains were collected from various laboratories and deposited at the International
574 Center for Microbial Resources-Bacterial Pathogens (CIRM-BP,
575 https://www6.inrae.fr/cirm_eng/BRC-collection-and-catalogue/CIRM-BP) (Table S1). The majority
576 of them (n=100) were isolated between 2007 and 2017 from diseased birds in 16 broiler farms located
577 in Brittany, France and were provided by Labofarm (Loudéac). Other poultry strains were isolated in
578 Poland (n=5), Belgium (n=1), and the United States (n=6). Six strains from human infections were
579 isolated in France (n=3), Belgium (n=2), and Germany (n=1). The source and the original name of the

580 strains from abroad is indicated in Table S1. Additional details are available in the supplemental
581 material.

582

583 *Genome sequencing and analysis*

584 All genomic DNA was subjected to random shotgun library preparation using the TruSeq DNA PCR-
585 Free kit (Illumina). Ready-to-load libraries were sequenced on Illumina Miseq or HiSeq 3000
586 platforms (Illumina) at GeT-PlaGe (Toulouse, France) and HiSeq 2500 platform at Eurofins
587 Genomics (Germany) using 150 bp paired-end chemistry. DNA of fourteen isolates was also
588 sequenced using Oxford Nanopore Technology platforms. Preparation of libraries and sequencing
589 were performed at the GeT-PlaGe core facility (INRAE Toulouse) or at MetaGenoPolis (INRAE
590 Jouy-en-Josas) according to the manufacturer's instructions. Additional details are available in the
591 supplemental material.

592 The 104 genomes with only Illumina reads were assembled using RiboSeed v0.4.73 (90). RiboSeed uses a
593 reference genome to resolve ribosomal RNA operons and globally improve whole genome assembly.
594 Assemblies were performed using NCTC 12421 (# NZ_LS483306) as reference genome for rRNA
595 operons, using SPAdes v3.13.0 (91) as assembler in "careful" mode using k values of 21, 33, 55, 77 and
596 99. The 14 genomes with Illumina and Nanopore reads were performed using Unicycler 0.4.4 (92), an
597 assembly pipeline for bacterial genomes that uses SPAdes for short read assembly Miniasm and Racon for
598 long read assemblies and polishing. Unicycler was launched with default parameters.

599 Genome annotation was conducted with Prokka v1.12 (93). First, coding DNA sequences were identified
600 on contigs longer than 200 bp by Prodigal v2.6.1 (94), which penalized CDSs shorter than 250 bp in order
601 to filter out false positives. CDSs were first annotated (--proteins Prokka parameter) using a protein
602 bank extracted from all the *Enterococcus* complete genomes in RefSeq (4198 genomes retrieved in
603 April, 2020). Annotation from hits with an e-value cut-off of 10⁻⁹ and 80% coverage were

604 transferred. CDSs with no hits on this bank were annotated using Prokka default workflow and
605 databanks.

606

607 *Pan-genome analysis and phylogenomic tree construction*

608 Pan-genome analysis was performed by comparing 118 *de novo* sequenced genomes of *E. cecorum*
609 and 30 public genomes from NCBI with N50 above 20 kb (January 2021). One reference genome was
610 available on the NCBI nucleotide database as NCTC 12421. Protein clustering was performed by
611 Roary (95) v-3.12.0 with 94% of identity, a “percentage of isolates a gene must be in to be core” of
612 100%, and the parameter “without split paralogs”. Genes classified as core were genes present in all
613 148 genomes. Accessory genes were all other genes present in 147 or fewer genomes. The gene
614 accumulation curves were produced with ggplot2 (96) from Roary analysis. The phylogenomic
615 analysis was performed using the *E. cecorum* core-genome. The 1,206 core genes of *E. cecorum* were
616 aligned using a codon aware alignment produced by PRANK (v170427); an unrooted tree was then
617 constructed using the BioNJ algorithm (97) in SeaView (v4.2) (98), using the Jukes and Cantor
618 distance and 1,000 bootstrap replicates. Clades were determined using the Jukes and Cantor distance
619 between aligned core-genes of less than 0.021 and a bootstrap value greater than 75%.

620

621 *Acquired antimicrobial resistance genes search*

622 ARGs research was performed using the ResFinder (v2.1) (99) tool and database (2019-04-26) for
623 90% of gene identity and 60% of coverage. BLASTN was used to detect the *bcr*-like gene (*uppP_2*)
624 and to compare the *vanA* locus with pVEF3 of from *E. faecium* 01_233 (34). Positive hits had at least
625 90% nucleotide identity and 60% coverage. GenoPlotR (v0.8.11) was used to visualize BLASTN
626 results having > 90% identity (34).

627

628 *ICE, GI, and Prophage detection*

629 ICEs and IMEs were detected in the eleven complete genomes and the two large contigs of genome
630 CIRMBP-1320 using ICEscreen (<https://icescreen.migale.inrae.fr>) and then inspected visually for
631 delineation. Genomic islands corresponded to large insertion of more than 10 CDSs resulting in a
632 synteny break between two genomes. Prophage prediction was performed using the prophage
633 detection tools PHASTER (PHAge Search Tool Enhanced Release) (100) and VIBRANT (Virus
634 Identification By iterative ANnotation) (101). Only predicted prophages with prediction scoring
635 ≥ 100 with PHASTER or VIBRANT were retained and manually inspected to determine the
636 attachment and integration sites in reference to the NCTC12421 genome (Accession NZ_LS483306).
637 PHASTER was further used to identify the most similar phage genomes.

638
639 *Hierarchical clustering*
640 Estimated marginal mean of biofilm and adhesion to collagen biovolumes, and serum growth indexes
641 were adjusted for experiment and strain factors using a linear model with the "emmeans" R package
642 (1.4). Strains with a similar Euclidian distance between estimated marginal means were grouped
643 using a hierarchical clustering algorithm with average linkage. Clusters of strains were defined by
644 cutting dynamically the dendrogram, using the DynamicTreeCut R package (1.63-1) (102).

645
646 *Genome wide association study (GWAS)*
647 GWAS analyses were performed using TreeWas (1.0) (103) to identify genetic loci (SNP and gene
648 presence/absence) associated with clade membership (clade A, B, C, D or E), clinical origin (clinical
649 and non-clinical poultry isolates and clinical human isolates), biofilm robustness (as binary strong
650 values versus others, as binary weak values versus others and phenotypic groups obtained by
651 clustering), and collagen type II adhesion and/or growth in chicken serum (similarly as biofilm
652 robustness). Significant genetic loci corresponded to p-value less than or equal to 0.05 according to
653 terminal test.

654 A set of criteria was applied to select SNPs or genes of interest. Criteria applied to select clade-
655 specific SNPs were more stringent and only group-exclusive SNPs were retained (sensitivity = 1 or 0
656 and specificity = 1 or 0). Genes whose presence was associated with clade membership (clade A, C,
657 or E) or clinical origin (clinical and non-clinical poultry isolates, and clinical human isolates), biofilm
658 robustness, collagen type II adhesion, or growth in chicken serum had sensitivity and specificity
659 scores greater than 0.66. In addition, genes whose absence was associated with clade membership or
660 clinical origin, biofilm robustness, collagen type II adhesion, or growth in chicken serum, had
661 sensitivity and specificity scores below 0.33.

662

663 *Data availability.*

664 All genomic data have been deposited in the EMBL ENA database under the project number
665 ERP135100. Accession numbers of raw reads and assembled genomes are available in Table S2A.

666

667 **Acknowledgements**

668 The authors thank Drs L. Borst (North Carolina State University, USA), B. Dolka (Warsaw
669 University of Life Sciences, Poland), E. Oswald (IRSD, Toulouse, France), J. Van Acker Acker (AZ
670 Sint-Lucas, Laboratory of Clinical microbiology, Ghent, Belgium), M. Vaneechoutte (Ghent
671 University Hospital, Belgium), and P. Warnke (Universitätsmedizin Rostock, Germany) for
672 generously providing strains used in this study. We thank Marie Bernard, Marine Gilles, and Arnaud
673 Marie for technical assistance. We are grateful to Julie Puterflam and Jean-Luc Guerin for fruitful
674 discussions and to Luc Devriese for the complementary information on strain NCTC12421. This
675 work has benefited from the facilities and expertise of the MIMA2 MET-GABI (INRAE,
676 AgroParisTech, 78352 Jouy-en-Josas, France; www6.jouy.inra.fr/mima2). We are grateful to the
677 INRAE MIGALE bioinformatics facility (MIGALE, INRAE, 2020. Migale bioinformatics Facility,

678 doi: 10.15454/1.5572390655343293E12) for providing help and/or computing and/or storage
679 resources. Migale is part of the Institut Français de Bioinformatique (ANR-11-INBS-0013). J.L. was
680 supported by a fellowship from ANSES and INRAE. This work was supported by the INRAE
681 metaprogramme GISA (project CecoType) and by the French Ministry of Agriculture (DGAL)
682 through the program Ecoantibio2 N°2018-180.
683

684 **REFERENCES**

- 685 1. Devriese LA, Dutta GN, Farrow JAE, Vandekerckhove A, Phillips BA. 1983. *Streptococcus*
686 *cecorum*, a new species isolated from chickens. Int J Syst Bacteriol 33:772-776.
- 687 2. Devriese LA, Homme J, Wijfels R, Haesebrouck F. 1991. Composition of the enterococcal and
688 streptococcal intestinal flora of poultry. J Appl Bacteriol 71:46-50.
- 689 3. Schreier J, Rautenschlein S, Jung A. 2021. Different virulence levels of *Enterococcus cecorum*
690 strains in experimentally infected meat-type chickens. PLoS One 16:e0259904.
- 691 4. Dolka B, Gołębiewska-Kosakowska M, Krajewski K, Kwieciński P, Nowak T, Zubstarski J,
692 Wilczyński J, Szeleszczuk P. 2017. Occurrence of *Enterococcus* spp. in poultry in Poland based
693 on 2014–2015 data. Med Weter 73:220-224.
- 694 5. Souillard R, Allain V, Toux JY, Lecaer V, Lahmar A, Tatone F, Amenna-Bernard A, Le
695 Bouquin S. 2019. Synthèse des pathologies aviaires observées en 2018 par le Réseau National
696 d'Observations Épidémiologiques en Aviculture (RNOEA). Bull Epid Santé Anim 88:1-5.
- 697 6. Aziz T, Barnes HJ. 2007. Is spondylitis an emerging disease in broiler breeders? World Poultry
698 12:44-45.
- 699 7. Kense MJ, Landman WJ. 2011. *Enterococcus cecorum* infections in broiler breeders and their
700 offspring: molecular epidemiology. Avian Pathol 40:603-12.
- 701 8. Stalker MJ, Brash ML, Weisz A, Ouckama RM, Slavic D. 2010. Arthritis and osteomyelitis
702 associated with *Enterococcus cecorum* infection in broiler and broiler breeder chickens in
703 Ontario, Canada. J Vet Diagn Invest 22:643-5.
- 704 9. Wood AM, MacKenzie G, McGiliveray NC, Brown L, Devriese LA, Baele M. 2002. Isolation of
705 *Enterococcus cecorum* from bone lesions in broiler chickens. Vet Rec 150:27.
- 706 10. Borst LB, Suyemoto MM, Sarsour AH, Harris MC, Martin MP, Strickland JD, Oviedo EO,
707 Barnes HJ. 2017. Pathogenesis of enterococcal spondylitis caused by *Enterococcus cecorum* in
708 broiler chickens. Vet Pathol 54:61-73.

- 709 11. Jung A, Rautenschlein S. 2014. Comprehensive report of an *Enterococcus cecorum* infection in a
710 broiler flock in Northern Germany. BMC Vet Res 10:311.
- 711 12. Jung A, Chen LR, Suyemoto MM, Barnes HJ, Borst LB. 2018. A review of *Enterococcus*
712 *cecorum* infection in poultry. Avian Dis 62:261-271.
- 713 13. Braga JFV, Martins NRS, Ecco R. 2018. Vertebral osteomyelitis in broilers: a review. Avian
714 Pathol 20:605-616.
- 715 14. Jung A, Metzner M, Ryll M. 2017. Comparison of pathogenic and non-pathogenic *Enterococcus*
716 *cecorum* strains from different animal species. BMC Microbiol 17:33.
- 717 15. Martin LT, Martin MP, Barnes HJ. 2011. Experimental reproduction of enterococcal spondylitis
718 in male broiler breeder chickens. Avian Dis 55:273-8.
- 719 16. Grund A, Rautenschlein S, Jung A. 2022. Detection of *Enterococcus cecorum* in the drinking
720 system of broiler chickens and examination of its potential to form biofilms. Europ Poult Sci
721 86:15.
- 722 17. De Herdt P, Defoort P, Van Steelant J, Swam H, Tanghe L, Van Goethem S, Vanrobaeys M.
723 2008. *Enterococcus cecorum* osteomyelitis and arthritis in broiler chickens. Vlaams
724 Diergeneeskd Tijdschr 78:44-48.
- 725 18. Grund A, Rautenschlein S, Jung A. 2020. Tenacity of *Enterococcus cecorum* at different
726 environmental conditions. J Appl Microbiol 130:1494-1507.
- 727 19. Borst LB, Suyemoto MM, Scholl EH, Fuller FJ, Barnes HJ. 2015. Comparative genomic analysis
728 identifies divergent genomic features of pathogenic *Enterococcus cecorum* including a type IC
729 CRISPR-Cas system, a capsule locus, an *epa-like* locus, and putative host tissue binding proteins.
730 PLoS One 10:e0121294.
- 731 20. Paganelli FL, Leavis HL, He S, van Sorge NM, Payré C, Lambeau G, Willems RJL, Rooijackers
732 SHM. 2018. Group IIA-secreted phospholipase A(2) in human serum kills commensal but not
733 clinical *Enterococcus faecium* isolates. Infect Immun 86.

- 734 21. Borst LB, Suyemoto MM, Keelara S, Dunningan SE, Guy JS, Barnes HJ. 2014. A chicken
735 embryo lethality assay for pathogenic *Enterococcus cecorum*. *Avian Dis* 58:244-8.
- 736 22. Jackson CR, Kariyawasam S, Borst LB, Frye JG, Barrett JB, Hiott LM, Woodley TA. 2015.
737 Antimicrobial resistance, virulence determinants and genetic profiles of clinical and nonclinical
738 *Enterococcus cecorum* from poultry. *Lett Appl Microbiol* 60:111-9.
- 739 23. Boerlin P, Nicholson V, Brash M, Slavic D, Boyen F, Sanei B, Butaye P. 2012. Diversity of
740 *Enterococcus cecorum* from chickens. *Vet Microbiol* 157:405-11.
- 741 24. Borst LB, Suyemoto MM, Robbins KM, Lyman RL, Martin MP, Barnes HJ. 2012. Molecular
742 epidemiology of *Enterococcus cecorum* isolates recovered from enterococcal spondylitis
743 outbreaks in the southeastern United States. *Avian Pathol* 41:479-85.
- 744 25. Dolka B, Chrobak-Chmiel D, Makrai L, Szeleszczuk P. 2016. Phenotypic and genotypic
745 characterization of *Enterococcus cecorum* strains associated with infections in poultry. *BMC Vet*
746 *Res* 12:129.
- 747 26. Robbins KM, Suyemoto MM, Lyman RL, Martin MP, Barnes HJ, Borst LB. 2012. An outbreak
748 and source investigation of enterococcal spondylitis in broilers caused by *Enterococcus cecorum*.
749 *Avian Dis* 56:768-73.
- 750 27. Wijetunge DS, Dunn P, Wallner-Pendleton E, Lintner V, Lu H, Kariyawasam S. 2012.
751 Fingerprinting of poultry isolates of *Enterococcus cecorum* using three molecular typing
752 methods. *J Vet Diagn Invest* 24:1166-71.
- 753 28. Sharma P, Gupta SK, Barrett JB, Hiott LM, Woodley TA, Kariyawasam S, Frye JG, Jackson CR.
754 2020. Comparison of antimicrobial resistance and pan-genome of clinical and non-clinical
755 *Enterococcus cecorum* from poultry using whole-genome sequencing. *Foods* 9:686.
- 756 29. Dolka B, Boyen F, Butaye P, Heidemann Olsen R, Naundrup Thofner IC, Christensen JP. 2015.
757 Draft genome sequences of two commensal *Enterococcus cecorum* strains isolated from chickens
758 in Belgium. *Genome Announc* 3.

- 759 30. Dolka B, Heidemann Olsen R, Naundrup Thofner IC, Christensen JP. 2015. Draft genome
760 sequences of five clinical *Enterococcus cecorum* strains isolated from different poultry species in
761 Poland. *Genome Announc* 3.
- 762 31. Dutta GN, Devriese LA. 1982. Susceptibility of fecal streptococci of poultry origin to nine
763 growth-promoting agents. *Appl Environ Microbiol* 44:832-7.
- 764 32. Yew WS, Gerlt JA. 2002. Utilization of L-ascorbate by *Escherichia coli* K-12: assignments of
765 functions to products of the *yjf-sga* and *yia-sgb* operons. *J Bacteriol* 184:302-6.
- 766 33. Linares D, Michaud P, Delort AM, Traikia M, Warrand J. 2011. Catabolism of L-ascorbate by
767 *Lactobacillus rhamnosus* GG. *J Agric Food Chem* 59:4140-7.
- 768 34. Nilsson O, Myrenas M, Agren J. 2016. Transferable genes putatively conferring elevated
769 minimum inhibitory concentrations of narasin in *Enterococcus faecium* from Swedish broilers.
770 *Vet Microbiol* 184:80-3.
- 771 35. Nilsson O, Greko C, Bengtsson B, Englund S. 2012. Genetic diversity among VRE isolates from
772 Swedish broilers with the coincidental finding of transferrable decreased susceptibility to
773 narasin. *J Appl Microbiol* 112:716-22.
- 774 36. Bellanger X, Payot S, Leblond-Bourget N, Guedon G. 2014. Conjugative and mobilizable
775 genomic islands in bacteria: evolution and diversity. *FEMS Microbiol Rev* 38:720-60.
- 776 37. Ambroset C, Coluzzi C, Guedon G, Devignes MD, Loux V, Lacroix T, Payot S, Leblond-
777 Bourget N. 2015. New insights into the classification and integration specificity of *Streptococcus*
778 integrative conjugative elements through extensive genome exploration. *Front Microbiol* 6:1483.
- 779 38. Coluzzi C, Guédon G, Devignes M-D, Ambroset C, Loux V, Lacroix T, Payot S, Leblond-
780 Bourget N. 2017. A glimpse into the world of integrative and mobilizable elements in
781 streptococci reveals an unexpected diversity and novel families of mobilization proteins. *Front*
782 *Microbiol* 8:443.

- 783 39. Cornuault JK, Petit MA, Mariadassou M, Benevides L, Moncaut E, Langella P, Sokol H, De
784 Paepe M. 2018. Phages infecting *Faecalibacterium prausnitzii* belong to novel viral genera that
785 help to decipher intestinal viromes. *Microbiome* 6:65.
- 786 40. Yoon BH, Chang HI. 2015. Genomic annotation for the temperate phage EFC-1, isolated from
787 *Enterococcus faecalis* KBL101. *Arch Virol* 160:601-4.
- 788 41. Díaz E, López R, García JL. 1992. EJ-1, a temperate bacteriophage of *Streptococcus pneumoniae*
789 with a Myoviridae morphotype. *J Bacteriol* 174:5516-25.
- 790 42. Mills S, Griffin C, O'Sullivan O, Coffey A, McAuliffe OE, Meijer WC, Serrano LM, Ross RP.
791 2011. A new phage on the 'Mozzarella' block: Bacteriophage 5093 shares a low level of
792 homology with other *Streptococcus thermophilus* phages. *Int Dairy J* 21:963-969.
- 793 43. Tettelin H, Massignani V, Cieslewicz MJ, Donati C, Medini D, Ward NL, Angiuoli SV, Crabtree
794 J, Jones AL, Durkin AS, Deboy RT, Davidsen TM, Mora M, Scarselli M, Margarit y Ros I,
795 Peterson JD, Hauser CR, Sundaram JP, Nelson WC, Madupu R, Brinkac LM, Dodson RJ,
796 Rosovitz MJ, Sullivan SA, Daugherty SC, Haft DH, Selengut J, Gwinn ML, Zhou L, Zafar N,
797 Khouri H, Radune D, Dimitrov G, Watkins K, O'Connor KJ, Smith S, Utterback TR, White O,
798 Rubens CE, Grandi G, Madoff LC, Kasper DL, Telford JL, Wessels MR, Rappuoli R, Fraser
799 CM. 2005. Genome analysis of multiple pathogenic isolates of *Streptococcus agalactiae*:
800 implications for the microbial "pan-genome". *Proc Natl Acad Sci USA* 102:13950-5.
- 801 44. McInerney JO, McNally A, O'Connell MJ. 2017. Why prokaryotes have pangenomes. *Nat*
802 *Microbiol* 2:17040.
- 803 45. Land M, Hauser L, Jun SR, Nookaew I, Leuze MR, Ahn TH, Karpinets T, Lund O, Kora G,
804 Wassenaar T, Poudel S, Ussery DW. 2015. Insights from 20 years of bacterial genome
805 sequencing. *Funct Integr Genomics* 15:141-61.

- 806 46. Touchon M, Perrin A, de Sousa JAM, Vangchhia B, Burn S, O'Brien CL, Denamur E, Gordon D,
807 Rocha EP. 2020. Phylogenetic background and habitat drive the genetic diversification of
808 *Escherichia coli*. PLoS Genet 16:e1008866.
- 809 47. Park CJ, Andam CP. 2020. Distinct but intertwined evolutionary histories of multiple *Salmonella*
810 *enterica* subspecies. mSystems 5.
- 811 48. Weinert LA, Chaudhuri RR, Wang J, Peters SE, Corander J, Jombart T, Baig A, Howell KJ,
812 Vehkala M, Välimäki N, Harris D, Chieu TT, Van Vinh Chau N, Campbell J, Schultsz C,
813 Parkhill J, Bentley SD, Langford PR, Rycroft AN, Wren BW, Farrar J, Baker S, Hoa NT, Holden
814 MT, Tucker AW, Maskell DJ. 2015. Genomic signatures of human and animal disease in the
815 zoonotic pathogen *Streptococcus suis*. Nat Commun 6:6740.
- 816 49. Weinert LA, Welch JJ. 2017. Why might bacterial pathogens have small genomes? Trends Ecol
817 Evol 32:936-947.
- 818 50. Rosinski-Chupin I, Sauvage E, Mairey B, Mangenot S, Ma L, Da Cunha V, Rusniok C, Bouchier
819 C, Barbe V, Glaser P. 2013. Reductive evolution in *Streptococcus agalactiae* and the emergence
820 of a host adapted lineage. BMC Genomics 14:252.
- 821 51. Merhej V, Georgiades K, Raoult D. 2013. Postgenomic analysis of bacterial pathogens repertoire
822 reveals genome reduction rather than virulence factors. Brief Funct Genomics 12:291-304.
- 823 52. Souillard R, Laurentie J, Kempf I, Le Caer V, Le Bouquin S, Serror P, Allain V. 2022.
824 Increasing incidence of *Enterococcus*-associated diseases in poultry in France over the past 15
825 years. Vet Microbiol 269:109426.
- 826 53. Hiemstra SJ, Ten Napel J. 2013. Study of the impact of genetic selection on the welfare of
827 chickens bred and kept for meat production (DG SANCO/2011/12254). J Final report of a
828 project commissioned by the European Commission.
- 829 54. Delaunay E, Abat C, Rolain JM. 2015. *Enterococcus cecorum* human infection, France. New
830 Microbes New Infect 7:50-1.

- 831 55. Stubljär D, Skvarc M. 2015. *Enterococcus cecorum* infection in two critically ill children and in
832 two adult septic patients. *Slov Vet Res* 52:39-44.
- 833 56. Brückner C, Straube E, Petersen I, Sachse S, Keller P, Layher F, Matziolis G, Spiegl U, Zajonz
834 D, Edel M, Roth A. 2019. Low-grade infections as a possible cause of arthrofibrosis after total
835 knee arthroplasty. *Patient Saf Surg* 13:1.
- 836 57. Lebreton F, Manson AL, Saavedra JT, Straub TJ, Earl AM, Gilmore MS. 2017. Tracing the
837 enterococci from paleozoic origins to the hospital. *Cell* 169:849-861.e13.
- 838 58. Khan A, Davlieva M, Panesso D, Rincon S, Miller WR, Diaz L, Reyes J, Cruz MR, Pemberton
839 O, Nguyen AH, Siegel SD, Planet PJ, Narechania A, Latorre M, Rios R, Singh KV, Ton-That H,
840 Garsin DA, Tran TT, Shamooy Y, Arias CA. 2019. Antimicrobial sensing coupled with cell
841 membrane remodeling mediates antibiotic resistance and virulence in *Enterococcus faecalis*.
842 *Proc Natl Acad Sci USA* 116:26925-32.
- 843 59. Frumkin I, Lajoie MJ, Gregg CJ, Hornung G, Church GM, Pilpel Y. 2018. Codon usage of
844 highly expressed genes affects proteome-wide translation efficiency. *Proc Natl Acad Sci USA*
845 115:E4940-E4949.
- 846 60. Ramos Y, Sansone S, Morales DK. 2021. Sugarcoating it: Enterococcal polysaccharides as key
847 modulators of host-pathogen interactions. *PLoS Pathog* 17:e1009822.
- 848 61. Thurlow LR, Thomas VC, Fleming SD, Hancock LE. 2009. *Enterococcus faecalis* capsular
849 polysaccharide serotypes C and D and their contributions to host innate immune evasion. *Infect*
850 *Immun* 77:5551-7.
- 851 62. Rohmer L, Hocquet D, Miller SI. 2011. Are pathogenic bacteria just looking for food?
852 Metabolism and microbial pathogenesis. *Trends Microbiol* 19:341-8.
- 853 63. Nogales J, Garmendia J. 2022. Bacterial metabolism and pathogenesis intimate intertwining:
854 time for metabolic modelling to come into action. *Microb Biotechnol* 15:95-102.

- 855 64. Cury J, Touchon M, Rocha EPC. 2017. Integrative and conjugative elements and their hosts:
856 composition, distribution and organization. *Nucleic Acids Res* 45:8943-8956.
- 857 65. Lao J, Guedon G, Lacroix T, Charron-Bourgoin F, Libante V, Loux V, Chiapello H, Payot S,
858 Leblond-Bourget N. 2020. Abundance, Diversity and Role of ICEs and IMEs in the Adaptation
859 of *Streptococcus salivarius* to the Environment. *Genes (Basel)* 11.
- 860 66. Couturier E, Rocha EP. 2006. Replication-associated gene dosage effects shape the genomes of
861 fast-growing bacteria but only for transcription and translation genes. *Mol Microbiol* 59:1506-18.
- 862 67. Lato DF, Golding GB. 2020. Spatial patterns of gene expression in bacterial genomes. *J Mol*
863 *Evol* 88:510-520.
- 864 68. Goessweiner-Mohr N, Arends K, Keller W, Grohmann E. 2014. Conjugation in Gram-Positive
865 bacteria. *Microbiol Spectr* 2:Plas-0004-2013.
- 866 69. Bhatti M, Laverde Gomez JA, Christie PJ. 2013. The expanding bacterial type IV secretion
867 lexicon. *Res Microbiol* 164:620-39.
- 868 70. Deng L, Spencer BL, Holmes JA, Mu R, Rego S, Weston TA, Hu Y, Sanches GF, Yoon S, Park
869 N, Nagao PE, Jenkinson HF, Thornton JA, Seo KS, Nobbs AH, Doran KS. 2019. The Group B
870 Streptococcal surface antigen I/II protein, BspC, interacts with host vimentin to promote
871 adherence to brain endothelium and inflammation during the pathogenesis of meningitis. *PLoS*
872 *Pathog* 15:e1007848.
- 873 71. Chuzeville S, Dramsi S, Madec JY, Haenni M, Payot S. 2015. Antigen I/II encoded by
874 integrative and conjugative elements of *Streptococcus agalactiae* and role in biofilm formation.
875 *Microb Pathog* 88:1-9.
- 876 72. Jurénas D, Fraikin N, Goormaghtigh F, Van Melderen L. 2022. Biology and evolution of
877 bacterial toxin-antitoxin systems. *Nat Rev Microbiol* 20:335–350.
- 878 73. Couvigny B, Lapaque N, Rigottier-Gois L, Guillot A, Chat S, Meylheuc T, Kulakauskas S,
879 Rohde M, Mistou MY, Renault P, Dore J, Briandet R, Serror P, Guedon E. 2017. Three

- 880 glycosylated serine-rich repeat proteins play a pivotal role in adhesion and colonization of the
881 pioneer commensal bacterium, *Streptococcus salivarius*. Environ Microbiol 19:3579-3594.
- 882 74. Latousakis D, MacKenzie DA, Telatin A, Juge N. 2020. Serine-rich repeat proteins from gut
883 microbes. Gut Microbes 11:102-117.
- 884 75. Kaufman JH, Terrizzano I, Nayar G, Seabolt E, Agarwal A, Slizovskiy IB, Noyes N. 2020.
885 Integrative and Conjugative Elements (ICE) and Associated Cargo Genes within and across
886 Hundreds of Bacterial Genera. bioRxiv
887 <https://doi.org/10.1101/2020.04.07.030320>.
- 888 76. Roberts MC, Schwarz S. 2016. Tetracycline and phenicol resistance genes and mechanisms:
889 importance for agriculture, the environment, and humans. J Environ Qual 45:576-92.
- 890 77. Lyras D, Adams V, Ballard SA, Teng WL, Howarth PM, Crellin PK, Bannam TL, Songer JG,
891 Rood JI. 2009. tISCpe8, an IS1595-family lincomycin resistance element located on a
892 conjugative plasmid in *Clostridium perfringens*. J Bacteriol 191:6345-51.
- 893 78. Han X, Du XD, Southey L, Bulach DM, Seemann T, Yan XX, Bannam TL, Rood JI. 2015.
894 Functional analysis of a bacitracin resistance determinant located on ICECp1, a novel Tn916-like
895 element from a conjugative plasmid in *Clostridium perfringens*. Antimicrob Agents Chemother
896 59:6855-65.
- 897 79. Chen M-Y, Lira F, Liang H-Q, Wu R-T, Duan J-H, Liao X-P, Martínez JL, Liu Y-H, Sun J.
898 2016. Multilevel selection of *bcrABDR*-mediated bacitracin resistance in *Enterococcus faecalis*
899 from chicken farms. Sci Rep 6:1-7.
- 900 80. Reynolds LJ, Anjum MF, Roberts AP. 2020. Detection of a novel, and likely ancestral, Tn916-
901 like element from a human saliva metagenomic library. Genes 11:548.
- 902 81. de Vries LE, Vallès Y, Agersø Y, Vaishampayan PA, García-Montaner A, Kuehl JV,
903 Christensen H, Barlow M, Francino MP. 2011. The gut as reservoir of antibiotic resistance:
904 microbial diversity of tetracycline resistance in mother and infant. PLOS ONE 6:e21644.

- 905 82. Harada T, Kawahara R, Kanki M, Taguchi M, Kumeda Y. 2012. Isolation and characterization of
906 *vanA* genotype vancomycin-resistant *Enterococcus cecorum* from retail poultry in Japan. Int J
907 Food Microbiol 153:372-7.
- 908 83. Singer RS, Porter LJ, Schrag NFD, Davies PR, Apley MD, Bjork K. 2020. Estimates of on-farm
909 antimicrobial usage in broiler chicken production in the United States, 2013-2017. Zoonoses
910 Public Health 67 Suppl 1:22-35.
- 911 84. Debaere O. 2016. Ecoantibio: premier plan de réduction des risques d'antibiorésistance en
912 médecine vétérinaire (2012-2016). Bull Acad Vet Fr 169:186-189.
- 913 85. Jouvin-Marche E, Carrara G, Pulcini C, Andremont A, Danan C, Couderc-Obert C, Lienhardt C,
914 Kieny M-P, Yazdanpanah YJTL. 2020. French research strategy to tackle antimicrobial
915 resistance. Lancet 395:1239-1241.
- 916 86. Urban D, Chevance A, Moulin G. 2021. Surveillance des ventes de médicaments vétérinaires
917 contenant des antibiotiques en France en 2020: Rapport annuel. Anses, Agence nationale de
918 sécurité sanitaire de l'alimentation, de l'environnement et du travail 1-92 doi:[https://hal-
919 anses.archives-ouvertes.fr/anses-03515142](https://hal-anses.archives-ouvertes.fr/anses-03515142).
- 920 87. Monteiro G, Rossi D, Valadares Jr E, Peres P, Braz R, Notário F, Gomes M, Silva R, Carrijo K,
921 Fonseca B. 2021. Lactic bacterium and *Bacillus* Sp. biofilms can decrease the viability of
922 *Salmonella gallinarum*, *Salmonella heidelberg*, *Campylobacter jejuni* and methicillin resistant
923 *Staphylococcus aureus* on different substrates. Braz J Poultry Sci 23.
- 924 88. Wideman RF, Al-Rubaye A, Kwon YM, Blankenship J, Lester H, Mitchell KN, Pevzner IY,
925 Lohrmann T, Schleifer J. 2015. Prophylactic administration of a combined prebiotic and
926 probiotic, or therapeutic administration of enrofloxacin, to reduce the incidence of bacterial
927 chondronecrosis with osteomyelitis in broilers. Poult Sci 94:25-36.

- 928 89. Luise D, Bosi P, Raff L, Amatucci L, Viridis S, Trevisi P. 2022. *Bacillus* spp. probiotic strains as
929 a potential tool for limiting the use of antibiotics, and improving the growth and health of pigs
930 and chickens. *Front Microbiol* 13.
- 931 90. Waters NR, Abram F, Brennan F, Holmes A, Pritchard L. 2018. riboSeed: leveraging prokaryotic
932 genomic architecture to assemble across ribosomal regions. *Nucleic Acids Res* 46:e68.
- 933 91. Bankevich A, Nurk S, Antipov D, Gurevich AA, Dvorkin M, Kulikov AS, Lesin VM, Nikolenko
934 SI, Pham S, Prjibelski AD, Pyshkin AV, Sirotkin AV, Vyahhi N, Tesler G, Alekseyev MA,
935 Pevzner PA. 2012. SPAdes: a new genome assembly algorithm and its applications to single-cell
936 sequencing. *J Comput Biol* 19:455-77.
- 937 92. Wick RR, Judd LM, Gorrie CL, Holt KE. 2017. Unicycler: Resolving bacterial genome
938 assemblies from short and long sequencing reads. *PLoS Comput Biol* 13:e1005595.
- 939 93. Ewels P, Magnusson M, Lundin S, Källner M. 2016. MultiQC: summarize analysis results for
940 multiple tools and samples in a single report. *Bioinformatics* 32:3047-8.
- 941 94. Hyatt D, Chen GL, Locascio PF, Land ML, Larimer FW, Hauser LJ. 2010. Prodigal: prokaryotic
942 gene recognition and translation initiation site identification. *BMC Bioinformatics* 11:119.
- 943 95. Page AJ, Cummins CA, Hunt M, Wong VK, Reuter S, Holden MT, Fookes M, Falush D, Keane
944 JA, Parkhill J. 2015. Roary: rapid large-scale prokaryote pan genome analysis. *Bioinformatics*
945 31:3691-3.
- 946 96. Wickham H. 2016. ggplot2: Elegant Graphics for Data Analysis. Springer-Verlag New York.
- 947 97. Gascuel O. 1997. BIONJ: an improved version of the NJ algorithm based on a simple model of
948 sequence data. *Mol Biol Evol* 14:685-95.
- 949 98. Gouy M, Guindon S, Gascuel O, evolution. 2010. SeaView version 4: a multiplatform graphical
950 user interface for sequence alignment and phylogenetic tree building. *J Molecular biology*
951 27:221-224.

- 952 99. Zankari E, Hasman H, Cosentino S, Vestergaard M, Rasmussen S, Lund O, Aarestrup FM,
953 Larsen MV. 2012. Identification of acquired antimicrobial resistance genes. *J Antimicrob*
954 *Chemother* 67:2640-4.
- 955 100. Arndt D, Grant JR, Marcu A, Sajed T, Pon A, Liang Y, Wishart DS. 2016. PHASTER: a better,
956 faster version of the PHAST phage search tool. *Nucleic Acids Res* 44:W16-21.
- 957 101. Kieft K, Zhou Z, Anantharaman K. 2020. VIBRANT: automated recovery, annotation and
958 curation of microbial viruses, and evaluation of viral community function from genomic
959 sequences. *Microbiome* 8:90.
- 960 102. Langfelder P, Zhang B, Horvath S. 2008. Defining clusters from a hierarchical cluster tree: the
961 Dynamic Tree Cut package for R. *J Bioinformatics* 24:719-720.
- 962 103. Collins C, Didelot X. 2018. A phylogenetic method to perform genome-wide association studies
963 in microbes that accounts for population structure and recombination. *PLoS Comput Biol*
964 14:e1005958.
- 965

966 **FIGURE LEGENDS**

967 **Fig. 1: Pan-genome analysis of 148 *E. cecorum* genomes.** **A.** Accumulation curves of gene clusters
968 of the pan and core-genomes. Pan-genome size in black corresponds to the total number of gene
969 clusters against the number of genomes included. Core-genome size in red corresponds to the number
970 of gene clusters in common against the number of genomes included; numbers averaged on 1,000
971 randomized orders for genome addition. **B.** Gene frequency spectrum. Only one representative per
972 gene cluster is considered.

973
974 **Fig. 2: Phylogenetic tree and clinical status of 148 *E. cecorum* isolates.** Neighbor-joining (BioNJ)
975 tree built on pairwise distance between genomes. Internal circle: Clades A to E with subclades E1 to
976 E13 (colored strips). First external circle: Clinical status of isolates (black: clinical poultry isolates,
977 white: non-clinical poultry isolates, grey: clinical human isolates). Second external circle: geographic
978 origin (■: France, ●: Germany, ★: United States, ▲: Poland, ■: Belgium). Third external circle: year
979 of isolation. The name underlined in red corresponds to reference genome NCTC 12421.

980
981 **Fig. 3: Distribution of antimicrobial resistance genes in sequenced genomes.** Clade, geographic
982 origin (■: France, ●: Germany, ★: United States, ▲: Poland, ■: Belgium), isolation year and clinical
983 origin of sample (CH: clinical human, NCP: non-clinical poultry, CP: clinical poultry isolates) are
984 specified. Antibiotic families are represented by alternating grey blocks, from left to right:
985 tetracycline, MLS (macrolide, lincosamide, and streptogramin), aminoglycoside, glycopeptide, and
986 bacitracin. Black strips represent the presence of ARG and white ones the absence. Potential
987 multiresistant isolates (>2 ARGs to different families) are highlighted in grey.

988

989 **Fig. 4: Mobile genetic elements in complete *E. cecorum* genomes.** From inner to outer circle:
990 CIRMBP-1212, CIRMBP-1283, CIRMBP-1292, CIRMBP-1246, CIRMBP-1302, NCTC12421,
991 CIRMBP-1287, CIRMBP-1320, CIRMBP-1274, CIRMBP-1281, CIRMBP-1261, CIRMBP-1228.
992 Dotted lines on genome CIRMBP-1320 correspond to predicted junctions. Each colored rectangle
993 indicates the integration of an element according to the color legend. Hatching indicates a complex
994 genomic island. *dnaA*, *rpoE*, *rpoD* genes and *epa* and *cps* loci are indicated.

995
996 **Fig. 5: Distribution of phenotypic expression for biofilm robustness, adhesion to type II**
997 **collagen, and growth in chicken serum for 118 *E. cecorum* isolates.** Values for biofilm and
998 adhesion to collagen represent estimated marginal mean biovolumes. Values for growth in serum
999 represent estimated marginal mean of serum growth index calculated at 6 h (see supplemental
1000 material). Each bar corresponds to an isolate. Strains with similar phenotypic expression were
1001 grouped into clusters in grey color scale.

1002
1003 **Fig. 6. Comparison of virulence of selected *E. cecorum* isolates in a chicken embryo model of**
1004 **infection.** Kaplan–Meier survival plot of chicken embryos (n=15) infected with 13 different isolates
1005 of *E. cecorum*; strain name, inoculum size, and phylogenetic group are indicated. The log-rank
1006 (Mantel-Cox) test indicated significant differences between the positive control CIRMBP-1311 (SA2)
1007 and strains CIRMBP-1309 (CE3, p-value <0.0001), CIRMBP-1212 (p-value= 0.0007), CIRMBP-
1008 1281 (p-value = 0.0364), CIRMBP-1283 (p-value = 0.0035), CIRMBP-1287 (p-value = 0.0339),
1009 CIRMBP-1294 (p-value <0.0001), and CIRMBP-1320 (p-value <0.0001). Virulence of strains
1010 CIRMBP-1292, CIRMBP-1304, CIRMBP-1228, CIRMBP-1274, and CIRMBP-1302 was not
1011 significantly different from CIRMBP-1311. One representative experiment of two is shown.

1012 **SUPPLEMENTAL MATERIAL**

1013 **Supplemental methods**

1014

1015 **Table S1:** Metadata of strains sequenced in the study.

1016

1017 **Table S2: A:** *E. cecorum* genomes sequenced in this study and included in the comparative analysis.

1018 **B:** Non-redundant *E. cecorum* genomes available in the NCBI Data base included in the comparative
1019 analysis.

1020

1021 **Table S3:** Genes differentially distributed between clade E isolates and isolates of other clades.

1022

1023 **Table S4: A:** Genes differentially distributed between clinical and non-clinical poultry isolates or
1024 clinical human isolates. **B:** Table S4B: Proposed set of discriminant accessory genes.

1025

1026 **Table S5: A:** Transposon, ICE, IME and genomic islands detected in *E. cecorum* complete or high-
1027 quality genomes. **B:** Distribution of ICEs and genomic islands of 12 strains in all available *E.*
1028 *cecorum* genomes.

1029

1030 **Table S6: A:** Prophages predicted in *E. cecorum* draft genomes. **B:** *E. cecorum* draft genomes with
1031 no predicted prophages.

1032

1033 **Table S7:** Genes present in highly and intermediate virulent *E. cecorum* isolates in embryonated eggs
1034 and absent in the non-virulent isolates.

1035

1036 **Figure S1: Inversion in two genomes compared to reference genome.** A. Alignment of CIRMBP-
1037 1261 genome and NCTC 12421. B. Alignment of CIRMBP-1287 and NCTC 12421. Blue lines
1038 symbolize inversion in genomes.

1039
1040 **Figure S2: Pairwise genetic distances between the *E. cecorum* genomes.** Color scale goes from
1041 green for close genomes to red for distant genomes. Tree clades are framed with respective colors
1042 used on the phylogenetic tree. Sub-clades are framed in black.

1043
1044 **Figure S3: Alignment of the predicted capsule locus in the complete genomes.** Arrows are
1045 annotated CDSs on both elements. The grayscale shading represents regions of nucleotide sequence
1046 identity (100% to 94%) determined by BLASTN analysis. The number of isolates that share each type
1047 of locus, among the 117 other genomes in the study, is shown on the right.

1048
1049 **Figure S4: Vancomycin and narasin resistance operons alignment between CIRMBP-1294 and**
1050 ***E. faecium* plasmid, pVEF3.** Blue arrows are annotated CDSs on the both elements. Grey highlights
1051 represent 99% or more of identity in BLASTN. Frames indicate vancomycin resistance and narasin
1052 resistance operons.

1053

1054

Figure 1

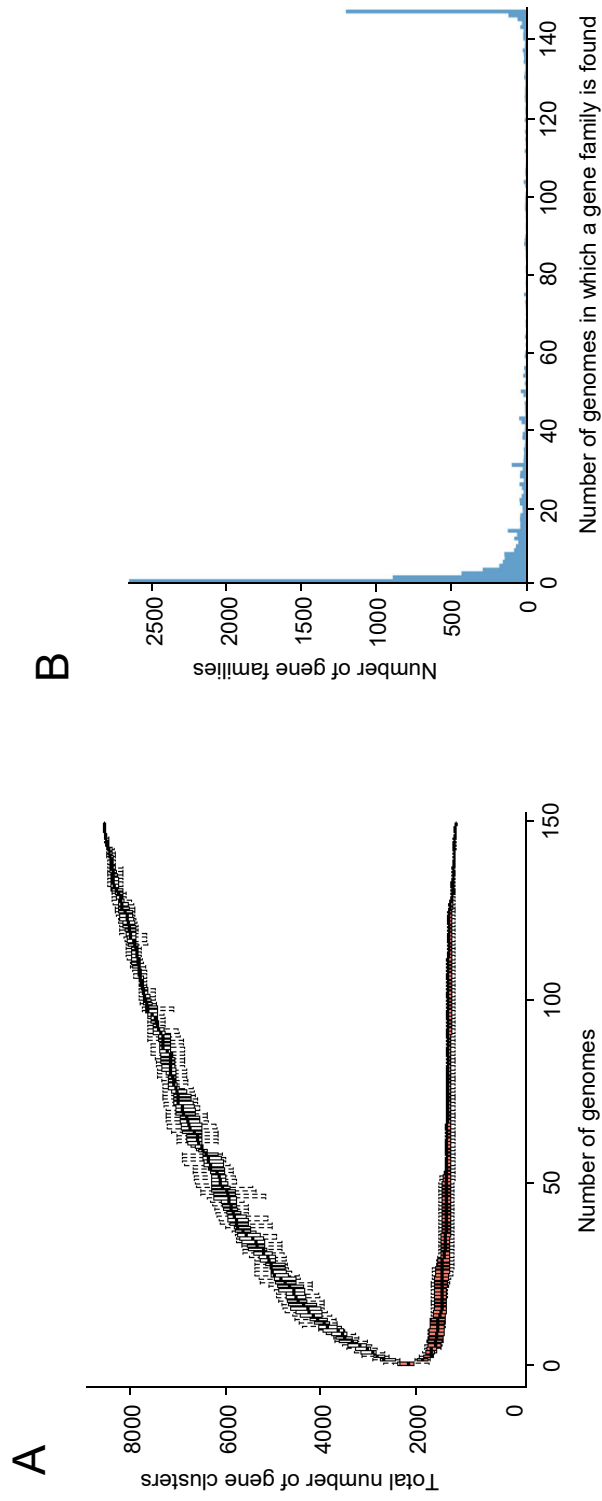


Fig. 1: Pan-genome analysis of 148 *E. cecorum* genomes. **A.** Accumulation curves of gene clusters of the pan and core-genomes. Pan-genome size in black corresponds to the total number of gene clusters against the number of genomes included. Core-genome size in red corresponds to the number of gene clusters in common against the number of genomes included; numbers averaged on 1,000 randomized orders for genome addition. **B.** Gene frequency spectrum. Only one representative per gene cluster is considered.

Figure 2

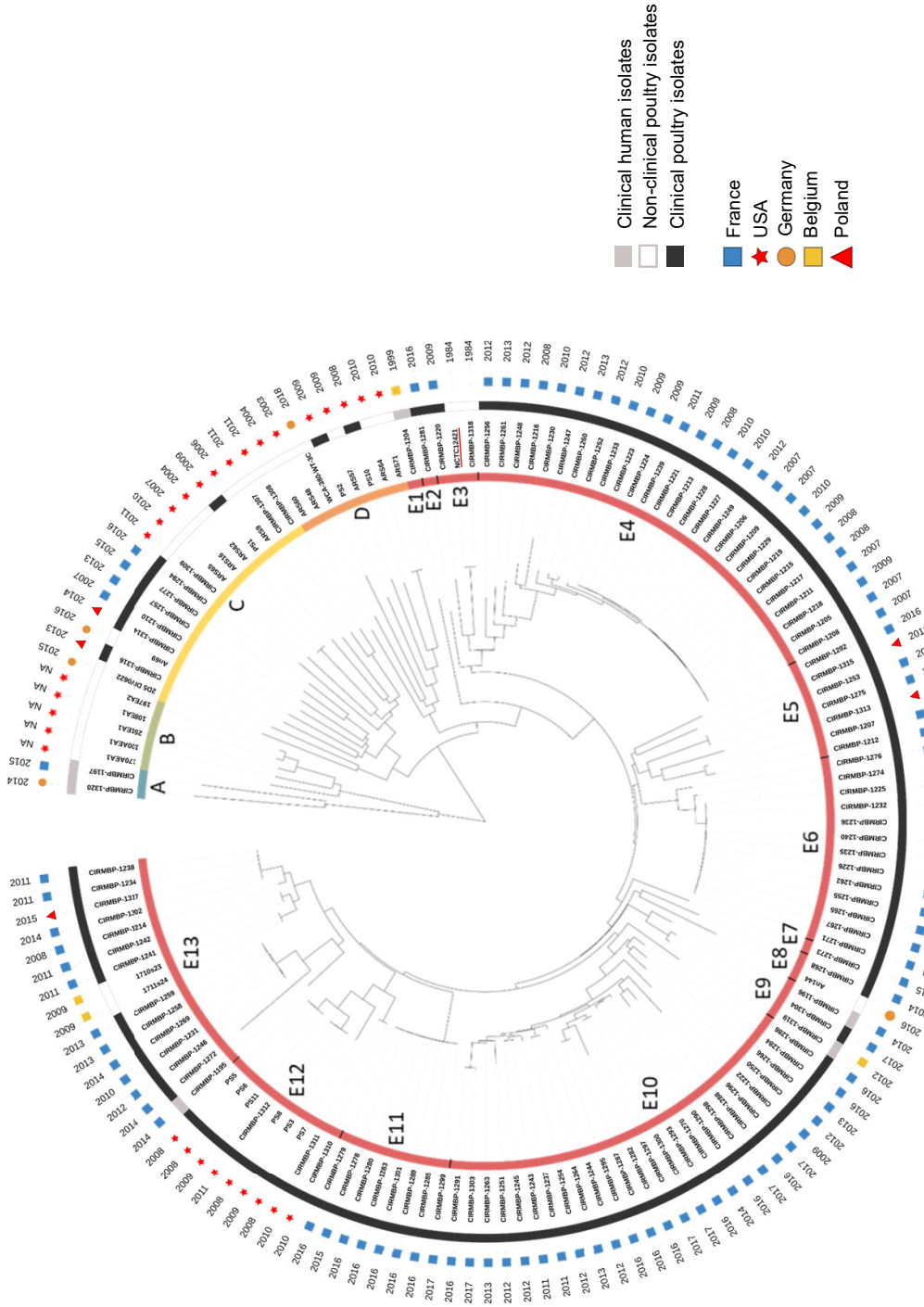


Fig. 2: Phylogenetic tree and clinical status of 148 *E. cecorum* isolates. Neighbor-joining (BioNJ) tree built on pairwise distance between genomes. Internal circle: Clades A to E with subclades E1 to E13 (colored strips). First external circle: Clinical status of isolates (black: clinical poultry isolates, white: non-clinical poultry isolates, grey: clinical human isolates). Second external circle: geographic origin (■ : France, ● : Germany, ★ : United States, ● : Poland, ■ : Belgium). Third external circle: year of isolation. The name underlined in red corresponds to reference genome NCTC 12421.

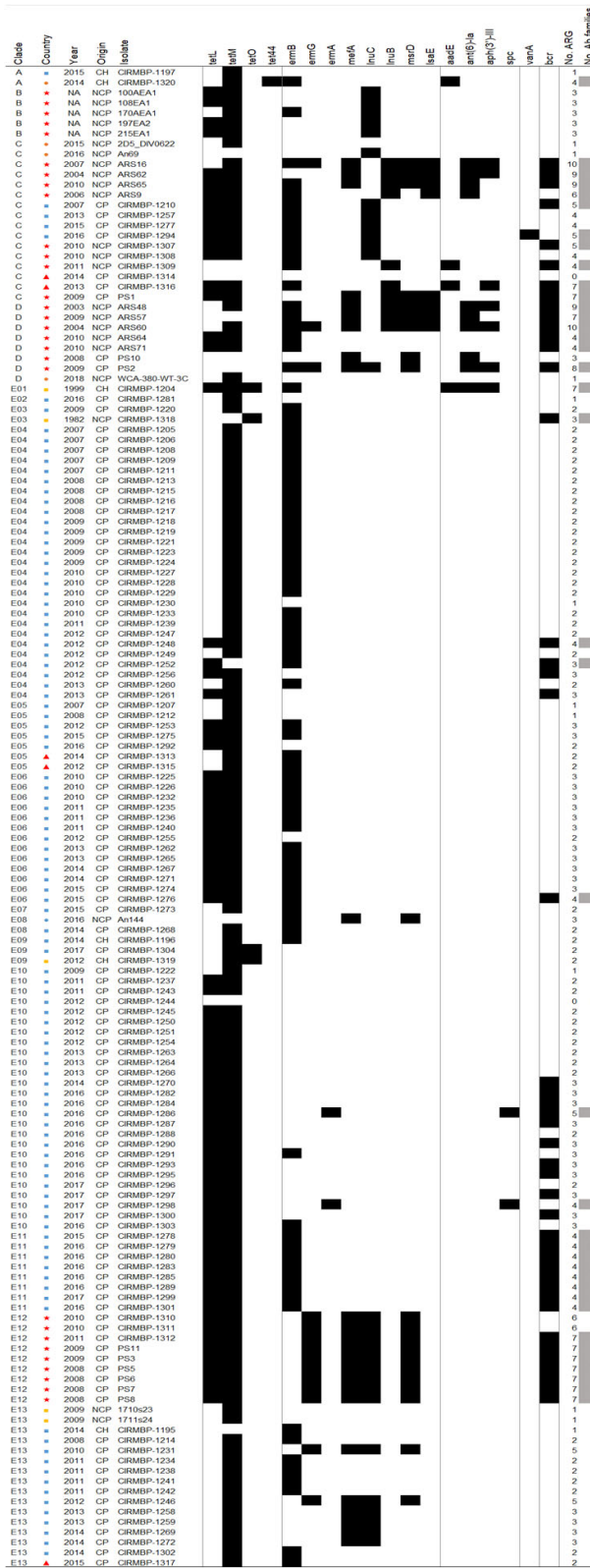


Figure 4

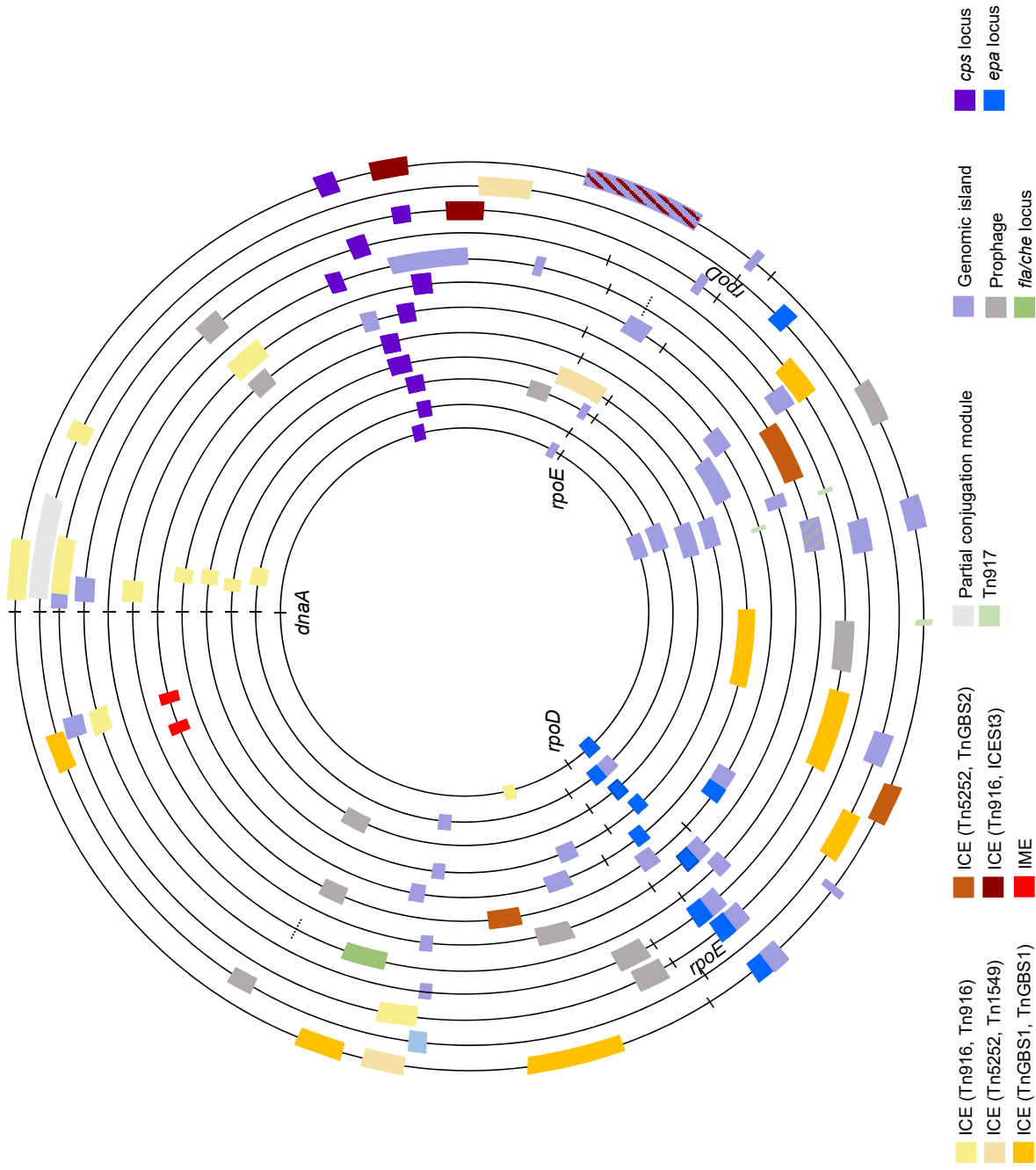


Fig. 4: Mobile genetic elements in complete *E. cecorum* genomes. From inner to outer circle: CIRM BP-1212, CIRM BP-1283, CIRM BP-1292, CIRM BP-1246, CIRM BP-1302, NCTC12421, CIRM BP-1287, CIRM BP-1320, CIRM BP-1274, CIRM BP-1281, CIRM BP-1261, CIRM BP-1228. Dotted lines on genome CIRM BP-1320 correspond to predicted junctions. Each colored rectangle indicates the integration of an element according to the color legend. Hatching indicates a complex genomic island. *dnaA*, *rpoE*, *rpoD* genes and *epa* and *cps* loci are indicated.

Figure 5

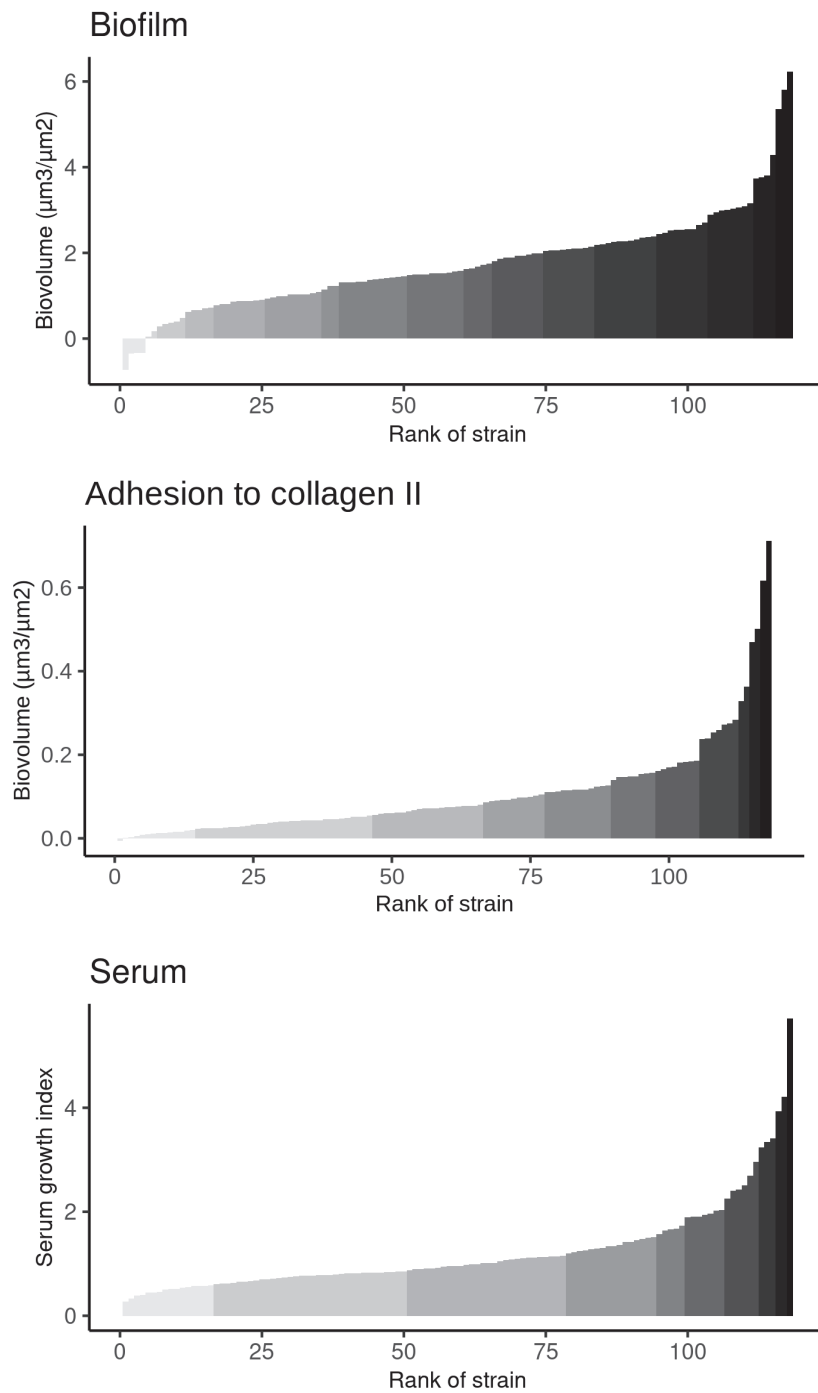


Fig. 5: Distribution of phenotypic expression for biofilm robustness, adhesion to type II collagen, and growth in chicken serum for 118 *E. cecorum* isolates. Values for biofilm and adhesion to collagen represent estimated marginal mean biovolumes. Values for growth in serum represent estimated marginal mean of serum growth index calculated at 6 h (see supplemental materiel). Each bar corresponds to an isolate. Strains with similar phenotypic expression were grouped into clusters in grey color scale.

Figure 6

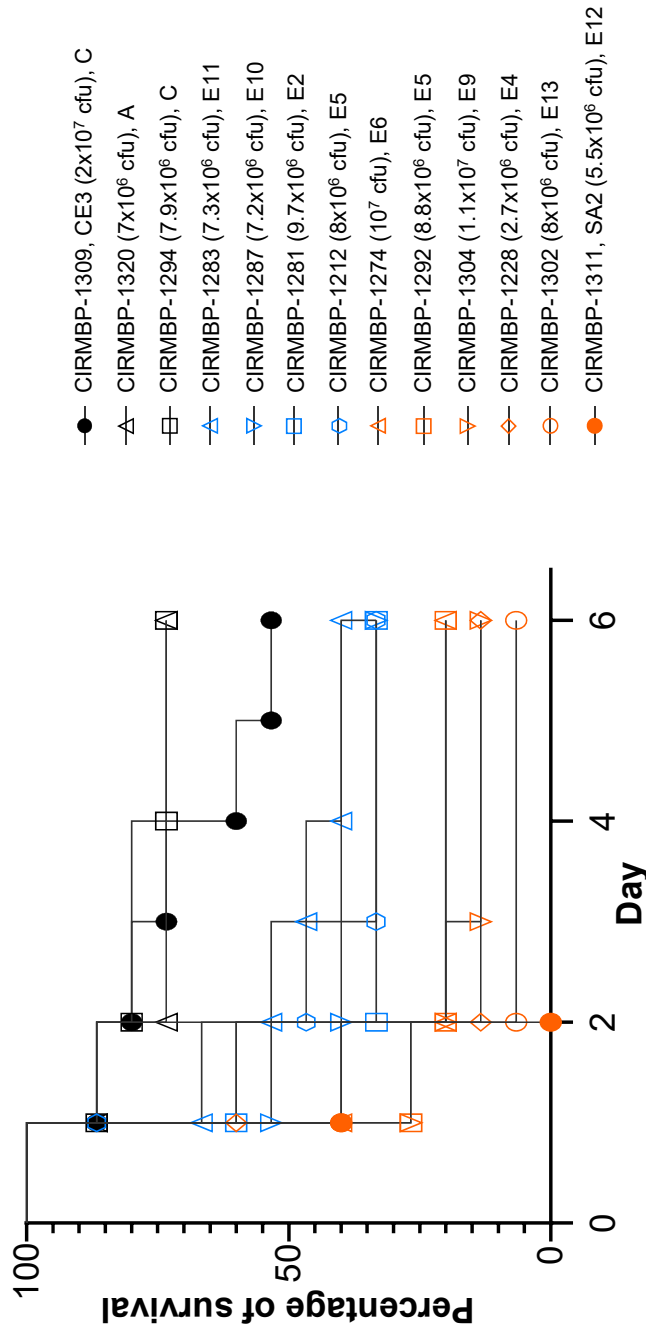


Fig. 6. Comparison of virulence of selected *E. cecorum* isolates in a chicken embryo model of infection. Kaplan–Meier survival plot of chicken embryos ($n=15$) infected with 13 different isolates of *E. cecorum*; strain name, inoculum size, and phylogenetic group are indicated. The log-rank (Mantel-Cox) test indicated significant differences between the positive control CIRMBP-1311 (SA2) and strains CIRMBP-1309 (CE3, p -value < 0.0001), CIRMBP-1212 (p -value = 0.0007), CIRMBP-1281 (p -value = 0.0364), CIRMBP-1283 (p -value = 0.0035), CIRMBP-1287 (p -value = 0.0339), CIRMBP-1294 (p -value < 0.0001), and CIRMBP-1320 (p -value < 0.0001). Virulence of strains CIRMBP-1292, CIRMBP-1304, CIRMBP-1228, CIRMBP-1274, and CIRMBP-1302 was not significantly different from CIRMBP-1311. One representative experiment of two is shown.